ICE, WATER AND ENERGY BALANCES OF SPARTAN GLACIER, ALEXANDER ISLAND

By A. W. JAMIESON *and* A. C. WAGER

ABSTRACT. Components of the energy balance of Spartan Glacier, Alexander Island, were measured during the period 1973–74. Conditions near the surface were dominated by gravity winds flowing down the glacier. There is no satisfactory theoretical treatment of this situation so estimates of sensible- and latent-heat exchange were necessarily crude. The accepted practice of measuring solar radiation with horizontally mounted radiometers gave misleading results because the glacier was not a diffuse scatterer at short wave-lengths. Approximately 50 per cent of the outgoing radiation was specularly reflected. The problem could be overcome by mounting the solarimeters parallel to the surface. Mass-balance measurements made between 1969 and 1974 showed that the glacier was decreasing by 1/500 of its mass per year, although errors in determining density caused uncertainties. Direct measurements of change of mass would enable the amount of energy used to melt ice to be determined accurately. The amount of sensible and latent heat could then be obtained as the residue of the energy balance.

SPARTAN GLACIER (lat. 71°03′S., long. 68°20′W; Fig. 1), on the east coast of Alexander Island, was selected for intensive study as part of the "Combined Balances Project" (UNESCO/IASH, 1970, 1973). The purpose of the project was to measure the ice, water and energy balances of glaciers in a wide range of environments as a contribution to the International Hydrological Decade, 1965–74. Spartan Glacier, with an area of 6·3 km.^{2}, was the most southerly glacier selected for study on a chain extending from Alaska through the Americas to the Antarctic Peninsula. It was chosen after an extensive search as being representative of Palmer Land. Other glaciers on the east coast of Alexander Island were mostly too large and too crevassed to be worked safely by a small party. Glaciers flowing into George VI Sound from Palmer Land were even larger and more dangerous. Spartan Glacier was the most suitable of the few small glaciers in the area. It was only 30 km. from the British Antarctic Survey station at Fossil Bluff and was easily accessible by tracked vehicles and aircraft. There were dangerous crevasses in only a few parts of the glacier. The drainage basin was better defined than for any other glacier in the area. It was proposed to run Spartan Glacier as a "special station" as defined in the "Combined Balances" guide (UNESCO/IASH, 1970, 1973). The function of such stations was to measure the components of the energy exchange at the glacier surface in addition to the ice and water balances. Existing techniques were to be tested and a check made on the absolute accuracy of the measurements. It was hoped to gain a better understanding of the physical processes involved.

On glaciers, the three balances are intimately connected because the energy balance largely determines the water balance, which in turn affects the mass balance. Accumulation measurements from September 1969 have been used in determining the ice balance. Measurements of run-off were made during the ablation season of 1973–74. Micro-meteorological measurements to determine the energy exchange began in 1972 and were made continuously for 2 years except for 2½ months during each winter when the glacier station was not occupied. The meteorological sensors, the recording system and the data-processing methods used are described in Appendices.

THE ICE BALANCE

Stake measurements

Accumulation

Fig. 2 presents maps of changes in surface level for the 4 budget years covered by observations of the stakes marked on Fig. 3. In the period from September 1969 to September 1970 there were only 41 stakes on the glacier and results were less certain than during the next 3 years.

Fig. 1. Spartan Glacier (centre foreground) and George VI Ice Shelf at the bottom of the picture. (Photograph by U.S. Navy for U.S. Geological Survey.)

Fig. 4 gives seasonal results for 1972 and 1973 when the measurements were made at approximately monthly intervals. The pattern of accumulation was not simple. The prevailing north-west wind, which accompanied all major snowfalls, was funnelled through the col at the head of the north-west lobe of the glacier. A standing wave probably caused areas of high velocity and low accumulation (A, B and C in Fig. 2) and an area D of low velocity and high accumulation. The ablation pattern (Fig. 4b and d) was determined more by sun angle and glacier slope than by altitude. Slopes facing the sun on the south side of the glacier showed most ablation. Measurements of accumulation could not be made near the snout because crevasses made access too dangerous. Therefore, the area north-east of the line B-B (Fig. 3) was omitted from the study area. Other areas too steep to permit measurement of accumulation have also been omitted from the study area. These areas were on the north side and at the head of the glacier. Maps of changes of surface level were made for the periods between stake measurements and changes in volume of the glacier were deduced (Fig. 5a).

Density

Ice at Spartan Glacier was formed by superimposition rather than by compaction of firn. Even in the winter, the snow was rarely more than 1 m. deep and it showed large variations in

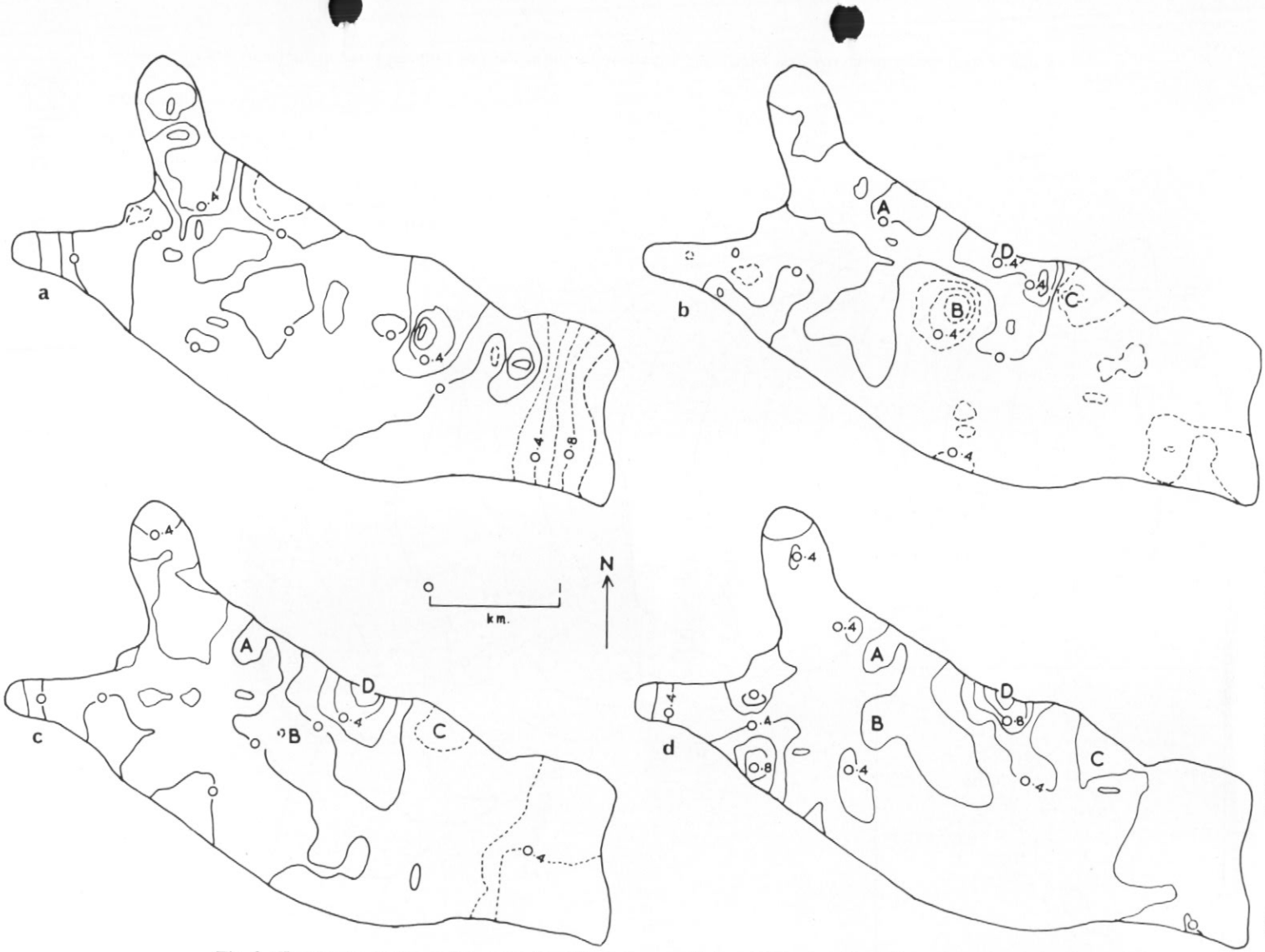

Fig. 2. Changes in glacier-surface level for 4 budget years. Interval between lines of equal accumulation is 0·2 m. Pecked lines indicate negative values (ablation).
a. 25 April 1970–28 April 1971; b. 28 April 1971–5 February 1972; c. 5 February 1972–28 February 1973; d. 28 February 1973–13 January 1974.

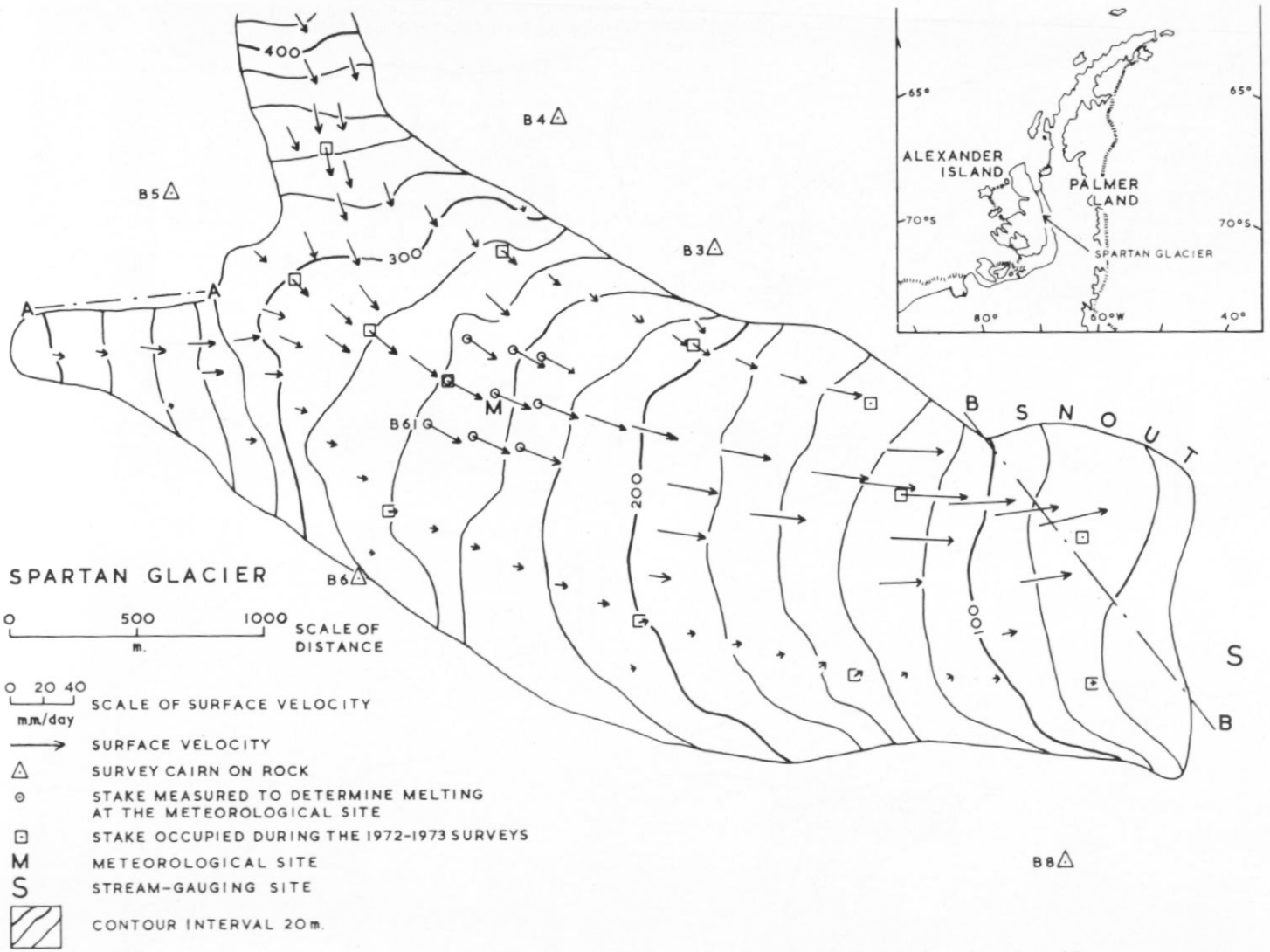

Fig. 3. Spartan Glacier. Flow into and out of the study area of the glacier was estimated across lines A and B.

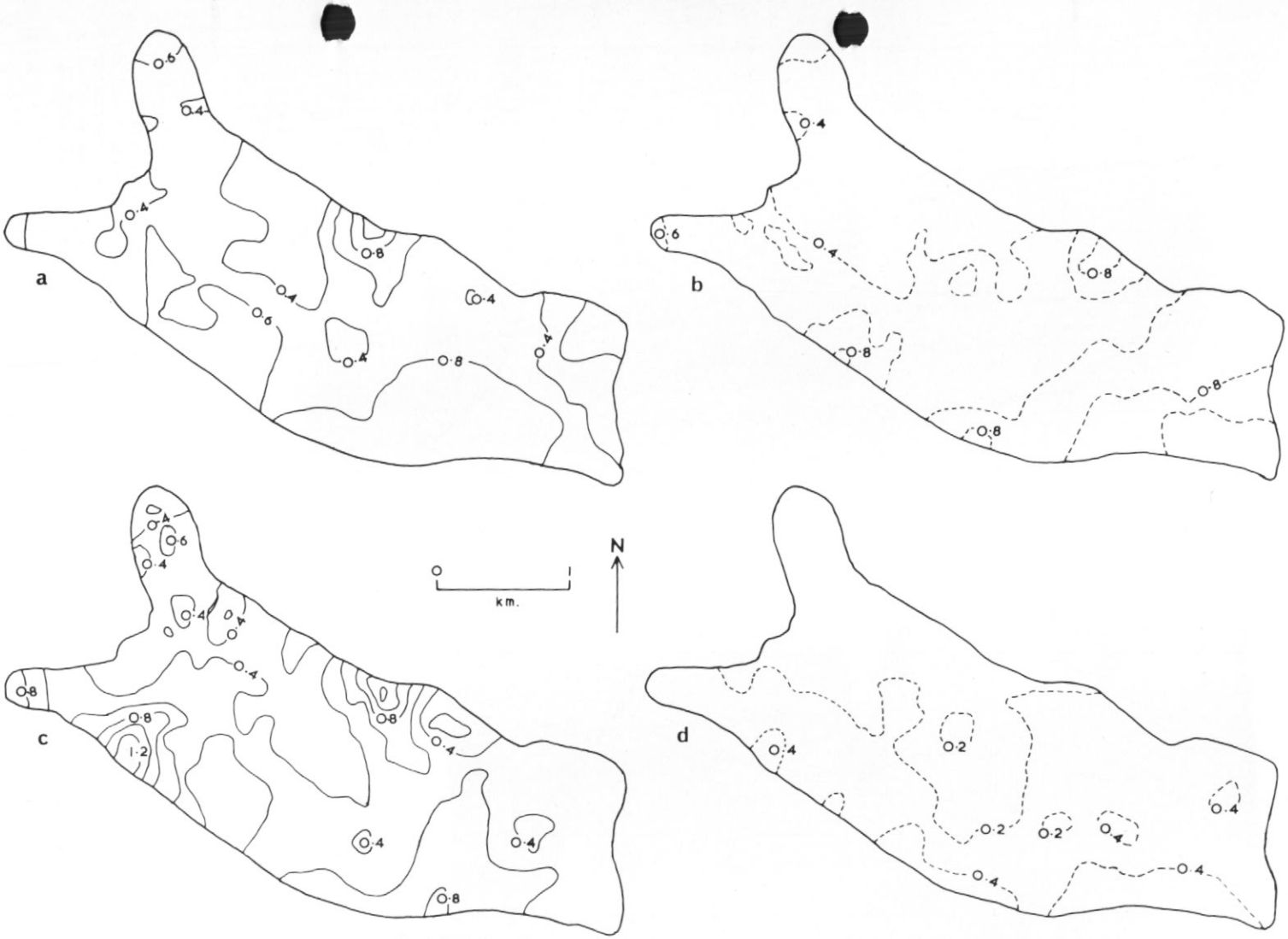

Fig. 4. Seasonal changes in glacier-surface level for 1972–73. Interval between lines of equal accumulation is 0·2 m. Pecked lines indicate negative values (ablation).
a. 5 February–12 November 1972; b. 12 November 1972–28 February 1973; c. 28 February–27 October 1973; d. 27 October 1973–13 January 1974.

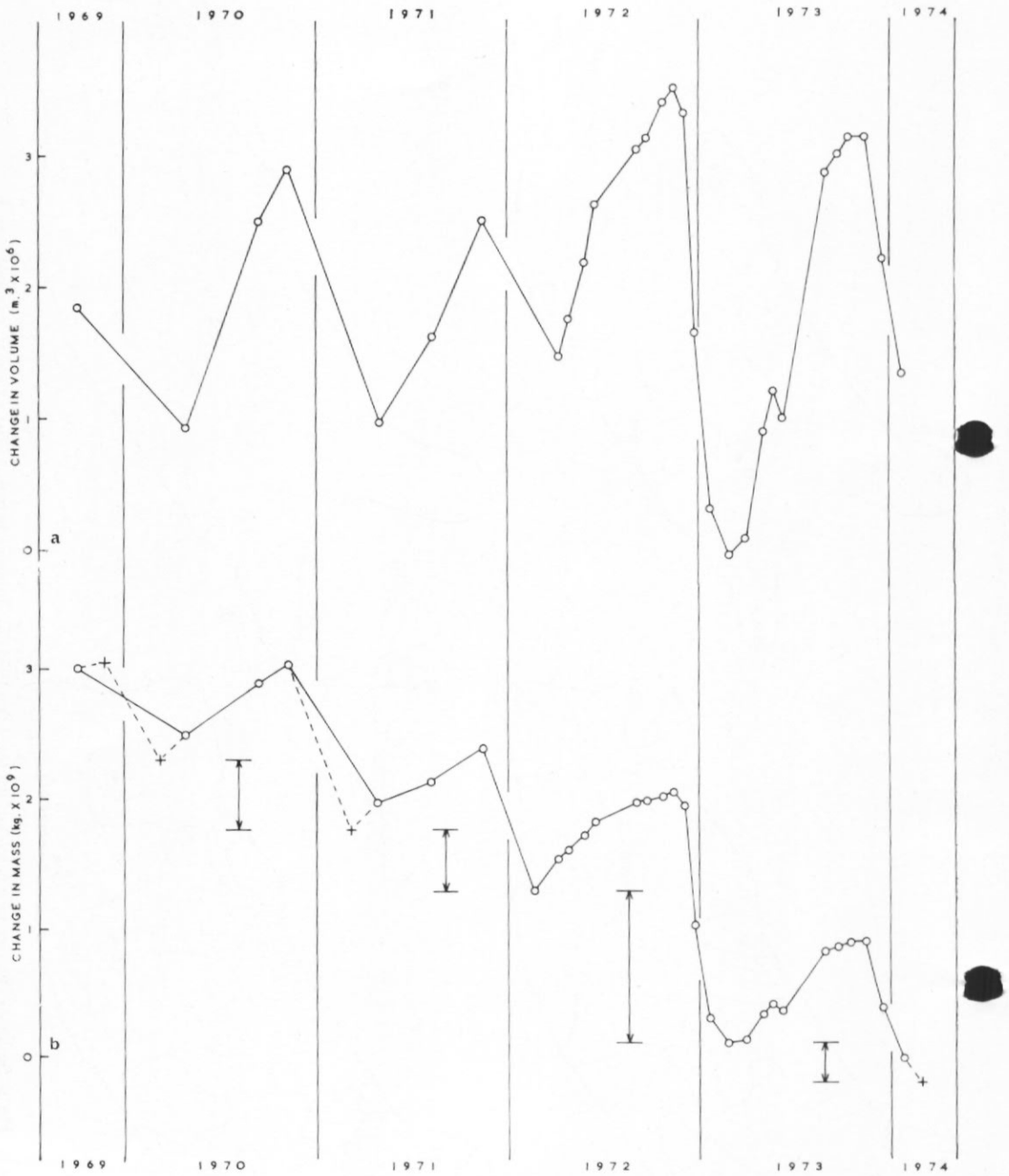

Fig. 5. a. Change of volume of snow and ice over the study area calculated from stake measurements.
b. Change of mass deduced from Fig. 5a, assuming a density of 250 kg. m.$^{-3}$ for accumulation and 550 kg. m.$^{-3}$ for ablation. Changes during budget years are indicated by the arrows. Circled dots represent the mass of the glacier with respect to the mass in September 1969. +symbols and pecked lines in 1970–71 are estimates for the ends of the accumulation and ablation seasons based on conditions in 1972–74.

density from place to place and at different depths. Thus repeated measurements of density in pits situated close together were unable to show the extent to which densities changed during the winter.

Summer snow cover over most of Spartan Glacier was 0·2–0·3 m. deep with a density of 300–400 kg m.$^{-3}$. Some of the incoming radiation was transmitted through this layer and partially melted the underlying ice. After a period of intense melt, the structure of the overlying snow layer became so irregular that its thickness and density could not be measured accurately. The upper part of the underlying ice was honeycombed. Changes in surface level were evidently caused by melting of both the snow and the underlying ice, followed by collapse of the honeycomb.

Changes in mass

Fig. 5b shows changes in mass at the surface of the glacier and these are summarized in Table I.

Glacier movement

Measurements

In November 1972 and November 1973 the positions of 13 stakes on the glacier were resected by observing angles to six rock stations (Fig. 3). Each of the remaining stakes was intersected from at least three resected stakes. Observation equations were formed from the angles by a computer program. Positions and velocities were then obtained by a least-squares solution of the equations. For most of the stakes, ice-surface velocities were determined with errors of <2 per cent in magnitude and 0·5° in azimuth. For a few stakes, where the intersections were poor, errors were within 5 per cent in magnitude and 15° in azimuth.

Flow of ice

The amount of ice which flowed into the study area, principally across A–A (Fig. 3), and the amount of ice which flowed out across B–B (Fig. 3) were estimated using maps of stake velocity (Fig. 6a) and ice thickness (Wager, 1976). The results indicate that 500 m.^{3} day^{-1} were flowing into the study area and 3,500 m.^{3} day $^{-1}$ were flowing out of the study area. Ice-surface velo-

TABLE I. SUMMARY OF CHANGES IN MASS AT THE SURFACE OF SPARTAN GLACIER

Year	*Date of end of season*		*Change in mass* ($\times 10^6$ kg.)		
	Accumulation	*Ablation*	*Accumulation* +	*Ablation* −	*Annual*
1969	30 September 1969 (20 November 1969)	25 April 1970 (20 February 1970)	—	510 (740)	—
1970	7 November 1970	28 April 1971 (20 February 1971)	530 (720)	1,060 (1,260)	−530 (−540)
1971	13 November 1971	19 February 1972	420 (620)	1,100	−780 (−680)
1972	12 November 1972	24 February 1973	760	1,950	−1,190
1973	14 November 1973	23 January 1974 (20 February 1974)	790	980 (1,180)	−190 (−390)

The changes in mass given in brackets are derived from values estimated on the dates in brackets shown as (+) in Fig. 5b.

cities (Fig. 3) show that ice flowed towards the north-east corner of the glacier. This area is now recognized as a true glacier snout (Fig. 7). It was earlier assumed that Spartan Glacier flowed into George VI Ice Shelf (Fig. 1) and measurements of ice depths (Fig. 8b) suggested that the two were continuous.

Subsequent measurements (Fig. 8a) showed that the ice shelf flowed almost due west to Alexander Island where there was a zone of intense bottom melting (Pearson and Rose, 1983). Spartan Glacier was isolated from the ice shelf by a line of pressure ridges.

The ice balance

Spartan Glacier is becoming smaller. On average, $0{\cdot}8 \times 10^6$ m.^{3} more ice melted in the study area each year than accumulated. 10^6 m.^{3} of ice per year also flowed from the study area to the snout, where it melted. The volume of the glacier, derived from the map of ice depths (Wager, 1982), was 800×10^6 m.^{3} and thus the glacier has decreased in size by 1/500 each year. If the present rate of decrease continues, there will no longer be a glacier in the valley in 500 years' time.

The Water Balance

The flow of a stream (S in Fig. 3) was measured during the ablation season 1973–74. This stream flowed into George VI Sound and drained the study area. A melting snow patch above a gully on the south side of the valley and an area of stagnant ice at the south-east corner of the glacier made a small contribution to the stream flow. The snout area, drained by streams flowing north, was separated from the study area by a watershed (Fig. 7). Measured run-off (Fig. 9) from 28 December 1973 to 2 February 1974 was 260×10^6 kg. Observed melting in the study area from 17 December 1973 to 23 January 1974 was 470×10^6 kg. The stream was also flowing between 17 and 28 December 1973, but it could not be approached because of deep slush. It would be difficult to refine the measurements. Melt water is retained by ice dams which form and break unpredictably. The time lag between melt and run-off is therefore variable.

The Energy Balance

Micro-meteorological parameters

The following micro-meteorological parameters (Fig. 10) were measured to determine the components of the energy exchange at the glacier surface. The sensors are described in Appendix A.

i. Incoming and reflected solar radiation was measured by Moll Gorczynski solarimeters. Net all-wave radiation was measured by a Funk radiometer.
ii. Wind speed was measured at five levels up to 5 m. using Porton anemometers.
iii. Temperature was measured at four levels in the air and at three levels in the ice. Platinum resistance thermometers measured the air temperature at 2 m. and the ice temperature 2 m. below the glacier surface. Intermediate temperatures were obtained using a chain of chromel-constantan thermojunctions as shown in Fig. 11. Temperature differences between these levels were measured by thermocouples formed by interconnecting the thermojunctions.
iv. Mixing ratio was measured directly at three levels up to 2 m. using Dewcels.

The sensors were connected to 24-channel chart recorders which sampled the output from each sensor every 72 sec. The response time of each sensor was increased to approximately 700 sec. so that rapid fluctuations in the output were attenuated and the traces on the charts could be followed more easily (Fig. 12).

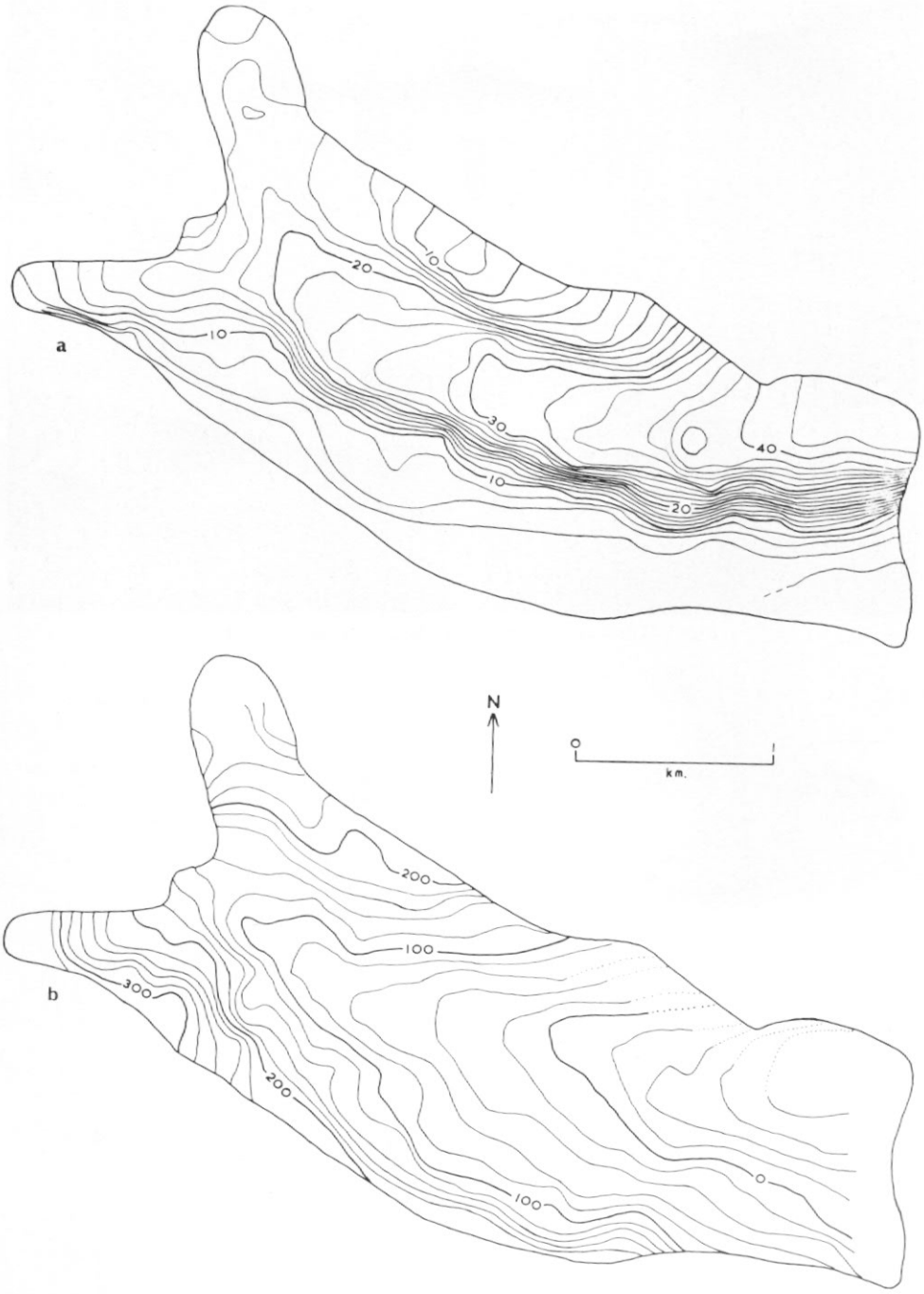

Fig. 6. a. Velocity of glacier surface (mm. day $^{-1}$). Interval between lines of equal velocity is 2 mm. day^{-1}.
b. Bedrock elevation. Interval between contours is 20 m. Contours below sea-level are pecked. Elevations obtained by radio echo-sounding (Wager, 1976).
The surface velocity is greatest over the deepest part of the valley.

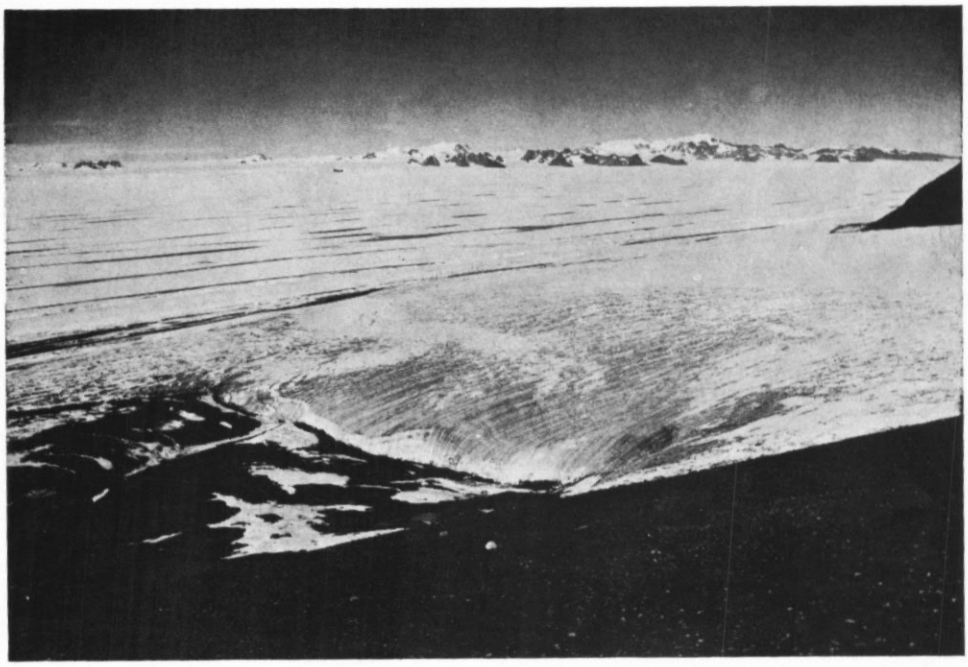

Fig. 7. The snout of Spartan Glacier looking south-east.

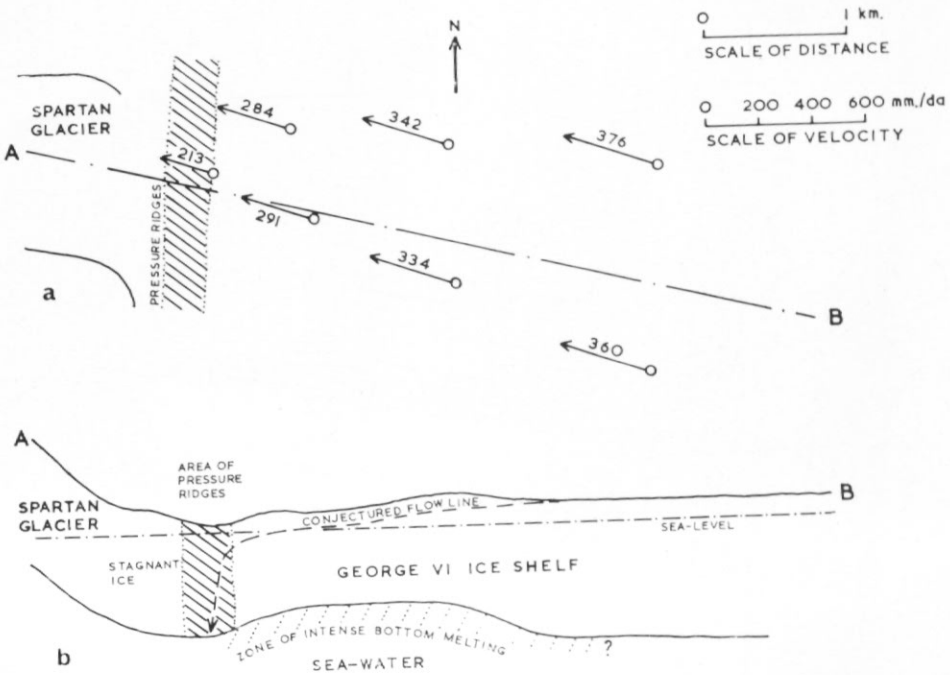

Fig. 8. a. Ice-surface velocities on George VI Ice Shelf determined by J. F. Bishop in 1974.
b. Section along line A–B in Fig. 8a. Ice depths were obtained by airborne radio echo-sounding (personal communication from B. M. E. Smith).

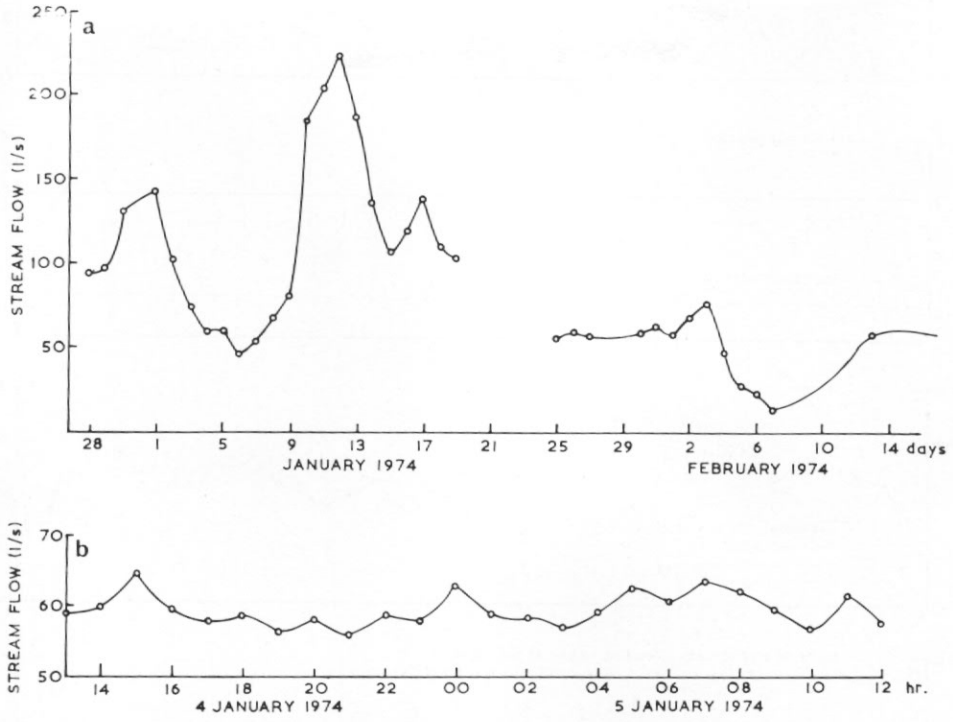

Fig. 9. a. Stream flow determined by measurements of the change in conductivity resulting from the dumping of a known amount of salt up-stream.
b. Diurnal variation of stream flow. There was a small lake at the bottom of the glacier which regulated the flow.

Radiation

Continuous records of incoming and reflected short-wave radiation and net all-wave radiation were obtained from the beginning of November 1973 to the end of January 1974. The radiative transfer of energy is a major component of the total energy exchange at a glacier surface. The net short-wave radiation must be measured correctly to obtain accurate results for the whole glacier. Many observers (Lister and Taylor, 1961; Streten and Wendler, 1968; Holmgren, 1971) measured the vertical components of the incident and reflected short-wave radiation with radiometers mounted horizontally. Indeed, it has been emphasized in the UNESCO/IASH (1973) guide that radiation should be measured in this way. In this section it is shown that for a sloping glacier surface this produces misleading results.

Apparent short-wave albedo

The ratio of reflected to incoming short-wave radiation, which is the apparent albedo of the glacier surface, varied greatly with weather conditions (Fig. 13). On fine clear days the apparent albedo was very high (approximately 1) early in the morning, after which it decreased throughout the day to a relatively low value of about 0·5 in the evening. On overcast days, the apparent albedo was virtually constant, about 0·8 ($\pm$0·05), and there appeared to be little variation during the 3 months for which there are records of the albedo. On days when there was an abrupt change from overcast to clear conditions, the apparent albedo changed as abruptly from that typical of overcast conditions to that typical of clear conditions. This indicated that

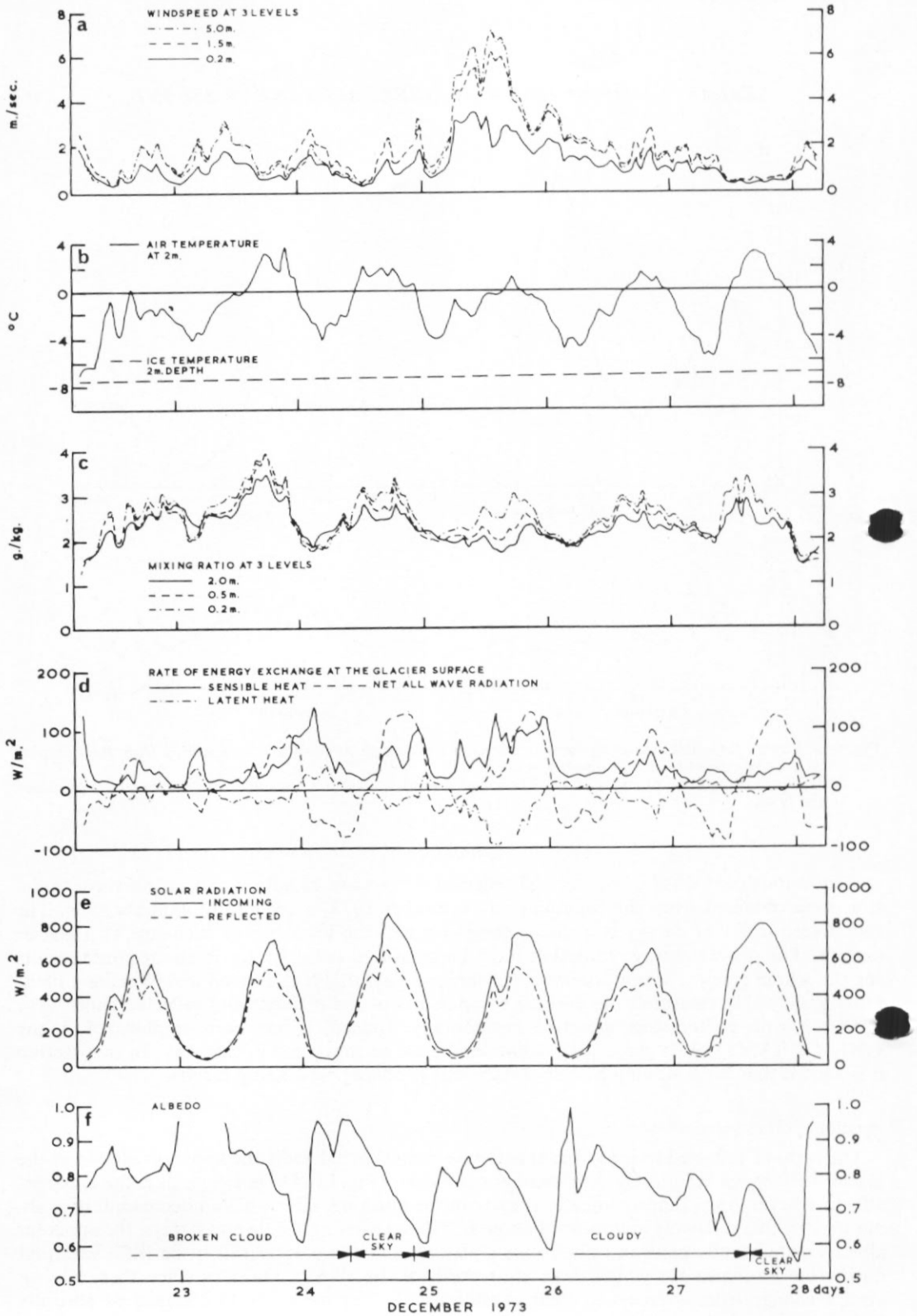

Fig. 10. Examples of hourly mean values of meteorological parameters and quantities derived from them.
a. Wind speed at three levels.
b. Air temperature and ice temperature.
c. Mixing ratio at three levels.
d. Rate of energy exchange at the glacier surface.
e. Incoming and reflected solar radiation.
f. Albedo.

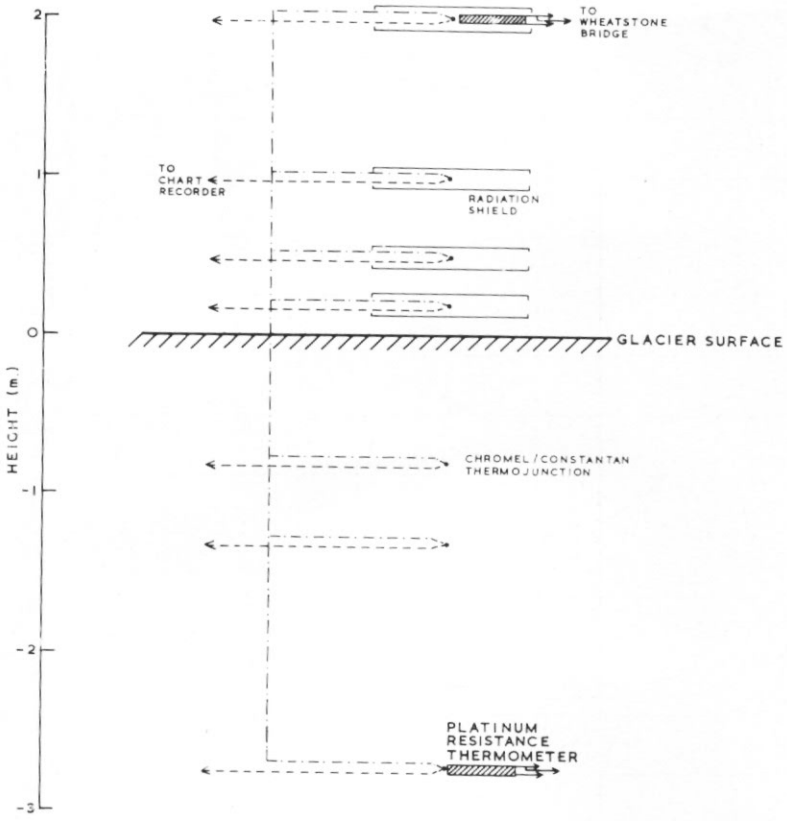

Fig. 11. Thermocouple chain and platinum resistance thermometers. The air sensors were embedded in paraffin wax in plastic tubes 9 cm. long and 2 cm. in diameter. Pecked lines indicate chromel wire, chain dotted lines indicate constantan wire.

variations in the apparent albedo were caused by changes in the cloud cover and not by changes in the physical condition of the glacier surface. A similar effect was noted by Streten and Wendler (1968) on Worthington Glacier, Alaska. They attributed it to specular reflection from the bare ice of the glacier surface.

Towards the end of summer the surface of Spartan Glacier became covered with a thin crust of ice about 1 mm. thick. An intense glare from the glacier surface was observed in the direction of the sun, indicating that specular reflection was occurring. LaChapelle (1969, p. 93–95) has described the phenomenon of *Firnspiegel* (firn mirror). The same variation in apparent albedo occurred in the Spartan Glacier records for mid-November 1973 when the crust had not formed. At this season the variation in albedo was probably due to the combined reflections from individual ice crystals.

Calculated short-wave albedo

Consider the reflection of radiation from a glacier surface (Fig. 14a). Let N W m.$^{-2}$ be the magnitude of the incident radiation; A be the total fraction of radiation (specular and diffuse) reflected from the surface; R be the specularly reflected fraction of the reflected radiation; α radians be the slope of the glacier in the direction of the sun; ϕ radians be the altitude of the sun.

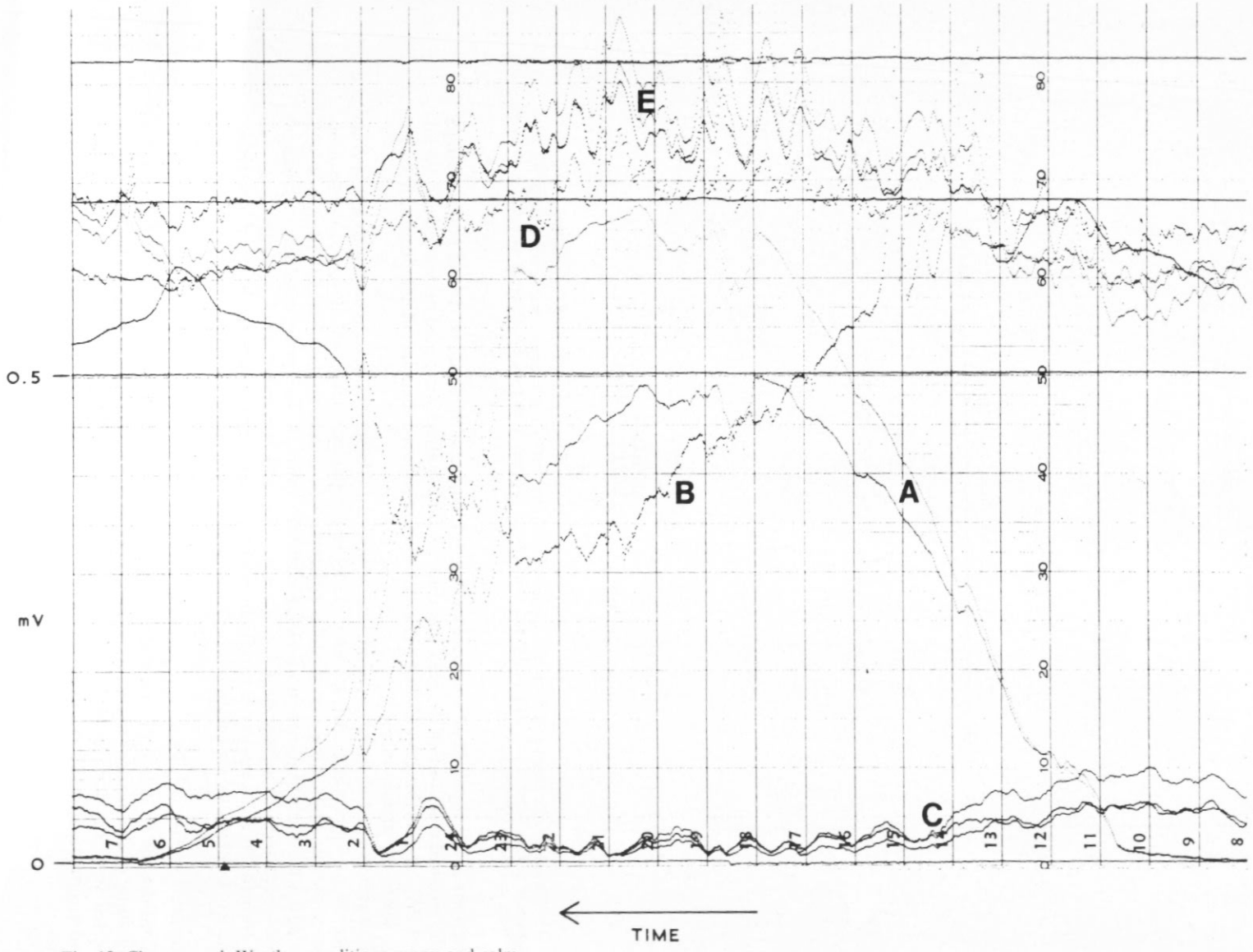

Fig. 12. Chart record. Weather conditions sunny and calm.
A. Incoming and reflected solar radiation. B. Net all-wave radiation. The zero point is 50 on the chart scale. Below 50 indicates incoming radiation. C. Wind speed at heights of 0·2, 1·5 and 5 m. D. Air temperature at 2 m. E. Mixing ratios at 0·2, 1 and 2 m.
Chart-recorder scale readings are related to measured parameters by calibration equations. Horizontal scale is 1 hr. per division.

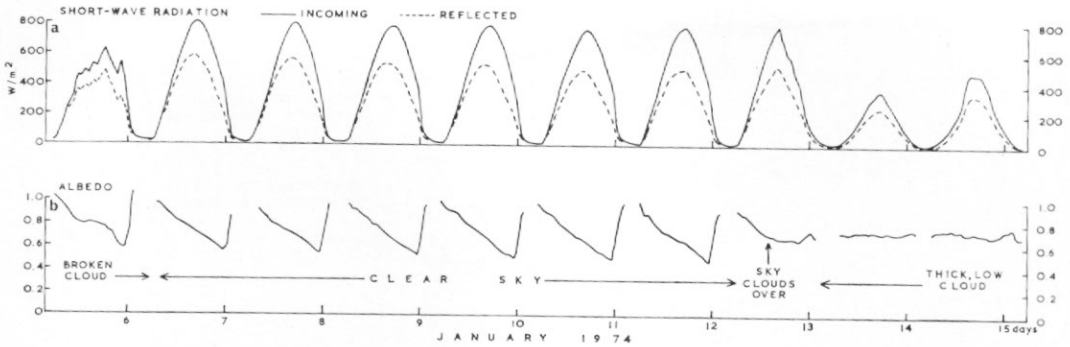

Fig. 13. Variation of intensity of short-wave radiation (a) and albedo (b) with the amount of cloud. The albedo calculated from the low radiation intensities measured at night is inaccurate and has been omitted.

The solarimeter measured the vertical component of the reflected radiation.

The specularly reflected contribution is

$$NAR \sin (\phi+2\alpha).$$

The magnitude of the diffuse contribution depends on the illumination of the surface, which is given by

$$N \sin (\phi+\alpha).$$

The diffuse contribution is therefore

$NA(1-R) \sin (\phi+\alpha)(1-k)$, where k is a constant error factor resulting from the fact that the radiometer was not mounted parallel to the glacier surface. Radiation reflected diffusely from the glacier surface was emitted within a hemisphere (Fig. 14b), and the diffusely reflected rays emitted into the shaded sector were not detected by the horizontally mounted solarimeter. The angle between the glacier surface and the horizontal sensing plate of the solarimeter was small (2·2°) and so, to a very close approximation, $k = 0$.

The radiation measured by the solarimeter was

$$NA\{R \sin (\phi+2\alpha)+[1-R] \sin (\phi+\alpha)\}$$

$$= NA\left\{2R \left(\cos \phi \cos \frac{3\alpha}{2} + \sin \phi \sin \frac{3\alpha}{2}\right) \sin \frac{\alpha}{2} + \sin (\phi+\alpha)\right\}.$$

Using the simplifications $\sin \phi \sin \frac{3\alpha}{2} \approx 0$, $\cos \frac{3\alpha}{2} \approx 1$, $\sin \alpha \approx \alpha$, where α is in radians, this reduces to

$$NA\{\sin \phi+\alpha (R+1) \cos \phi\}.$$

The upward-facing solarimeter measured the vertical component of the incident radiation given by

$$N \sin \phi,$$

and therefore the apparent albedo was

$$A\{1+\alpha (R+1) \cot \phi\},$$

which reduces to A for a horizontal surface ($\alpha = 0$). The apparent albedo calculated for two times of day when the sun altitude was equal is shown below in Table II. The fraction (R)

TABLE II. CALCULATED VALUES OF APPARENT ALBEDO

Date	*Sun altitude at 11.00 GMT and 22.00 GMT*	*Apparent albedo (sun due east) 11.00 GMT*	*Apparent albedo (sun due west) 22.00 GMT*	*R*
17 November 1973	21·2°	0·87	0·58	0·51
11 January 1974	23·9°	0·75	0·51	0·41

The value used for A was 0·8, the albedo on cloudy days.
The value used for α was 0·04 radians (2·2°).

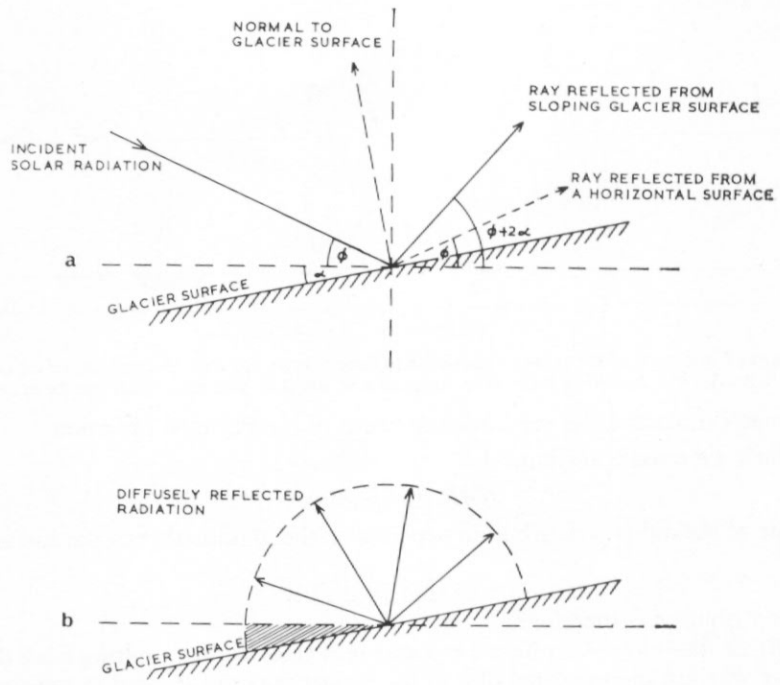

Fig. 14. a. Specular reflection from the glacier surface.
b. Diffuse reflection from the glacier surface.
Solarimeter does not detect radiation emitted into the shaded sector.

of specularly reflected radiation is estimated, using measured values of the albedo.

Had the solarimeters been mounted parallel with the glacier surface, the analysis would be simple. Incident radiation becomes

$$N \sin (\phi+\alpha),$$

and reflected radiation becomes

$$\underset{\text{(specular)}}{NAR \sin (\phi+\alpha)} + \underset{\text{(diffuse)}}{NA\,(1-R) \sin (\phi+\alpha)}.$$

The albedo is then simply A.

Net radiation

Snow and clouds behave as black bodies at long wave-lengths. This means that long-wave radiation is diffuse because the sources are extended objects. The slope angle of the glacier does not affect the long-wave albedo. To summarize, radiometers used to measure the net radiation flux on glaciers have generally been mounted horizontally. If short-wave radiation is being reflected specularly from the surface, the measurements are misleading because the reflected short-wave radiation is over- or under-estimated depending on the time of day. Accurate measurements of the components normal to the glacier surface could be obtained by mounting the radiometers parallel to the glacier surface. It would then be simple to obtain the normal components at any other point on the glacier provided that the surface slope is known.

The net radiation term was calculated for 5-day periods and is plotted on Fig. 19. Because Spartan Glacier is orientated almost exactly east–west and because the slope of the glacier is

fairly uniform, the under-estimation of net radiation in the morning is probably compensated by over-estimation in the afternoon.

Heat storage

The change with time in the heat stored in the surface layers of the glacier is given by

$$\int_{-h_i}^{0}\{T_1(h)H_1(h)-T_2(h)H_2(h)\}\mathrm{d}h, \tag{1}$$

where $T_1(h)$, $T_2(h)$ are the temperature profiles as functions of depth at two separate times. $H_1(h)$ and $H_2(h)$ are the corresponding profiles of heat capacity per unit volume, and h is the depth.

$$H_1(h) = c\rho_1(h),$$

where ρ_1 is the ice density as a function of depth, and c is the specific heat of ice. -10 m. was used for the lower limit of integration, $-h_i$. This was the depth below which seasonal variations in temperature were negligible. Temperatures in the ice were recorded continuously at depths of 0·5, 1 and 2 m. The temperature at 10 m. depth was $-8°$ C. Profiles were fitted to the daily mean temperatures. The form used was

$$e^{\lambda h}(a_0+a_1h+a_2h^2+a_3h^3) = t-t_{10}, \tag{2}$$

where a_0, a_1, a_2 and a_3 are coefficients, t is the temperature at depth h, t_{10} is the 10 m. temperature and λ is the damping coefficient. These profiles are similar to those obtained for a temperature wave travelling through a solid. The polynomial part of the equation was related to the history of the surface temperature. When the 2 m. air temperature was below zero, it was used as an approximation to the surface temperature and, when the air temperature was positive, the surface temperature was taken to be zero.

Typical profiles are shown in Fig. 15, which illustrates the warming up of the glacier. Profiles using different values of λ were derived using the same temperatures. When λ was changed by 0·05, the value of the integral changed by only 1 per cent despite a marked change in the shape of the profile. It was considered that a value for λ of 1·25 gave the most realistic profiles.

Calculation and errors

Snow-density profiles were measured at approximately monthly intervals. There were 10–30 cm. of snow (density $\sim$ 300 kg. m.$^{-3}$) overlying glacier ice (density $\sim$ 900 kg. m.$^{-3}$). Changes in the heat stored were calculated for 5-day periods and are plotted in Fig. 19. From September 1973 to February 1974, the period for which there are reliable data, heat was almost always being stored in the glacier.

The density of the topmost layers was low, and thus the heat capacity was also low. If the difference between the 2 m. land surface temperatures was constant, the errors caused by approximating the surface temperature to the 2 m. air temperature cancel exactly. If the temperature difference changes by 1° C, the error in heat stored is approximately 10 per cent.

Turbulent exchange

Symbols

u Wind velocity.
u_* Friction velocity.
k von Karman's constant ($\sim$ 0·4).
z Height measured from glacier surface.

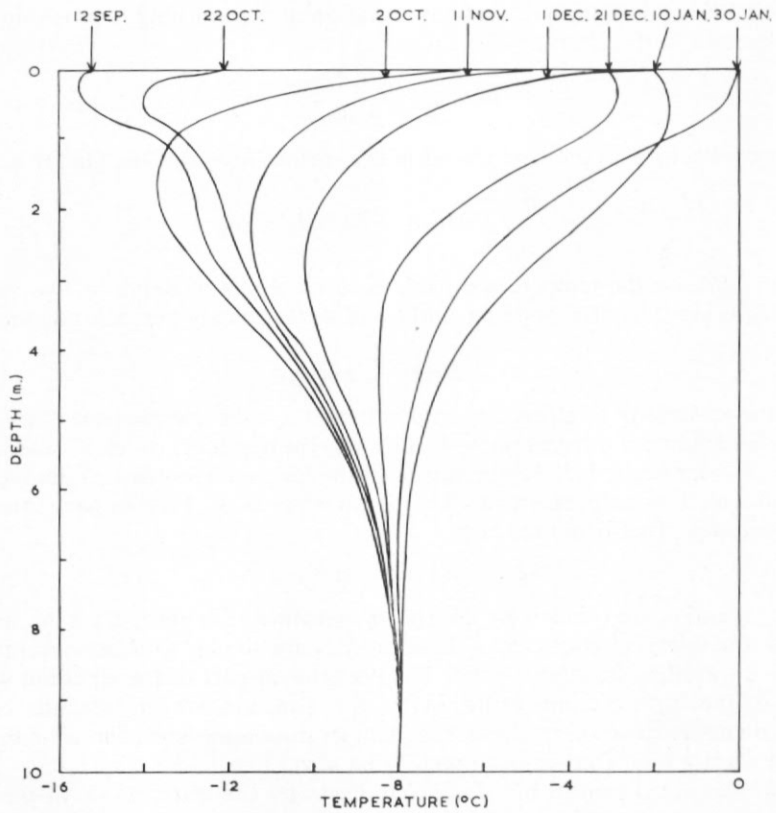

Fig. 15. Temperature profiles in the glacier during the period September 1973–January 1974. Measurements were made at depths of 0·5, 1, 2 and 10 m.

z_0 Roughness height.
β characterizes profiles produced by Deacon's law for unstable, neutral or stable atmospheric conditions.
g Acceleration due to gravity.
θ Temperature.
R_i Richardson number.
Γ Adiabatic lapse rate.
γ Expansion coefficient of air.
ζ Distance measured normal to the glacier surface.
ϕ Angle of slope of glacier surface.
K_H Eddy conductivity.
K_M Eddy viscosity.
ρ Density of air.
q Mixing ratio (weight of water vapour per unit weight of dry air).
c_p Specific heat of air at constant pressure.

Profiles

The transfer of heat to and from glacier surfaces by turbulent convection has been an enigma for many years. A number of studies (Lister and Taylor, 1961; Havens and others, 1965;

Dalrymple and others, 1966; Holmgren, 1971) have produced empirical results but little progress in understanding the basic principles of the process. In particular, there is no agreement about how the energy transferred can be estimated.

The basic equation of turbulent transfer

$$\frac{u}{u_*} = \frac{1}{k} \log_e \frac{z}{z_0} \tag{3}$$

was modified empirically by Deacon (1949) to explain deviations found experimentally in non-adiabatic atmospheric conditions.

Wind profiles on Spartan Glacier were examined and it was found that about 70 per cent of the profiles showed wind speed decreasing with height (Fig. 16a). These were not consistent with Deacon's wind-speed equation.

$$u = \frac{u_*}{k(1-\beta)} \left[\left(\frac{z}{z_0} \right)^{1-\beta} - 1 \right].$$

Measured temperatures (Fig. 16) did not give profiles consistent with the corresponding temperature equation. Lettau (1966, p. 8), de la Casinière (1974, p. 59) and Holmgren (1971, p. 11) found similar profiles with turning points. de la Casinière (1974, p. 59) attributed the turning points to the effect of surface undulations. He calculated the sensible heat flux, assuming that the profile above the turning point followed a logarithmic law.

Analysis of stability

Dalrymple and others (1966) analysed micro-meteorological measurements from the South Pole. They further extended Deacon's wind-speed equation by allowing β to vary with height (Dalrymple and others, 1966, p. 19–20). It is believed that in certain circumstances this involves unjustified assumptions. They characterized different profiles by modified Richardson numbers

$$R_i = \frac{g \Delta z}{\theta} \cdot \frac{\Delta \theta}{(\Delta u)^2}. \tag{4}$$

For profiles which followed Deacon's law, this was a reasonable approximation to the definition of the Richardson number in terms of derivatives

$$R_i = \frac{g}{\theta} \frac{\frac{\partial \theta}{\partial z} - \Gamma}{\left(\frac{\partial u}{\partial z} \right)^2}. \tag{5}$$

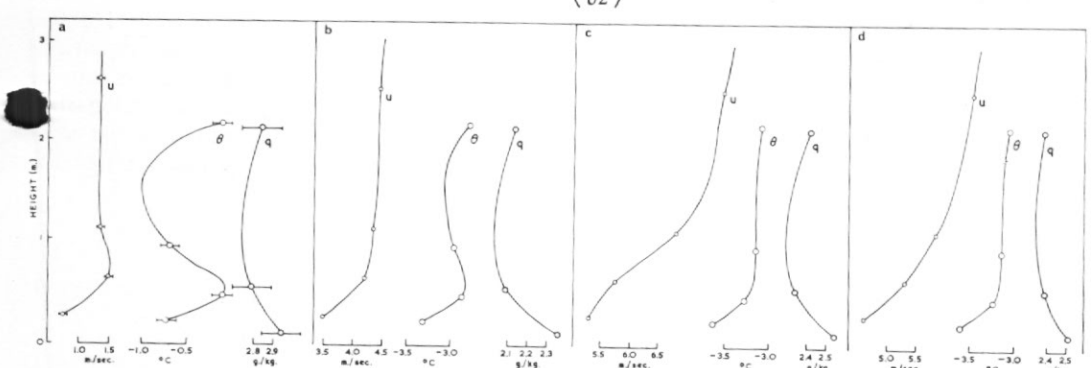

Fig. 16. Profiles of wind speed (u), temperature (θ) and mixing ratio (q) at
a. 15.00 GMT 2 December 1973; b. 22.00 GMT 2 December 1973; c. 01.00 GMT 3 December 1973; d. 03.00 GMT 3 December 1973.
They show the change in profile shapes with increasing wind speed from down-slope wind conditions to fully turbulent flow. Representative error bars are shown on only one diagram.

Richardson number profiles (Appendix C) were plotted for some of the Spartan Glacier data. For profiles which contained a turning value, $\frac{\partial u}{\partial z}$ was zero for a particular height. The Richardson number tended to infinity, since the numerator was non-zero. The sign depended on the sign of the numerator and was positive in most cases. The turning point may be interpreted as a boundary that prevents turbulent transfer. Equation (4) is of doubtful validity in cases where Δu is taken across a turning value in the profile.

Slope winds

An explanation for the discrepancies between profiles from Spartan Glacier and predictions from Deacon's theory was suggested by results obtained by Prandtl (1952). Prandtl derived the theoretical form of the wind-speed and temperature profiles close to a sloping surface in an area where the vertical temperature gradient was non-adiabatic.

$$\theta'(\zeta) = \theta_0' \cos \frac{\zeta}{l} \exp\left(-\frac{\zeta}{l}\right)$$

$$u(\zeta) = \theta_0' \left(\frac{g\gamma K_M}{BK_H}\right)^{\frac{1}{4}} \sin \frac{\zeta}{l} \exp\left(-\frac{\zeta}{l}\right),$$

where

$$l^4 = 4\left(\frac{K_M K_H}{g\gamma}\right) \frac{\operatorname{cosec}^2\phi}{B}.$$

These functions are shown in Fig. 17. Wind-speed profiles (Fig. 16a) measured at Spartan Glacier were similar. The temperature profiles did not show such similarities which indicates that the assumptions made by Prandtl were over-simplified.

Conditions at Spartan Glacier were determined largely by the down-slope wind, which appeared to be superimposed on a wind with a logarithmic velocity profile. This situation has been discussed in great detail by Holmgren (1971, p. 34), who reported differences of 10–40 per cent between the sensible heat flux calculated from the simple theory and from his equations.

The simple approach

Holmgren (1971, p. 37–38) expressed doubt about the validity of his equations. He could not test them because of the lack of precision in his measurements of temperature. He also implied that it would be impossible to refine the measurements sufficiently for the equations to be tested. There is no point in elaborating a theory beyond the point at which it can be tested. We have therefore calculated sensible- and latent-heat fluxes using the simple logarithmic profile (Equation (3)). These crude values are included only for comparison with the work of others, and not because it is believed that they represent meaningful components of the energy balance.

The equations (Lister and Taylor, 1961, p. 29) are

$$\text{(latent-heat flux)} = \frac{\rho k^2 u_2}{D}(q_2 - q_1) \tag{6}$$

$$\text{(sensible-heat flux)} = -\frac{\rho c_p k^2 u_2}{D}(\theta_2 - \theta_1), \tag{7}$$

where

$$D = \log_e \frac{z_2}{z_0} \log_e \frac{z_2}{z_1}.$$

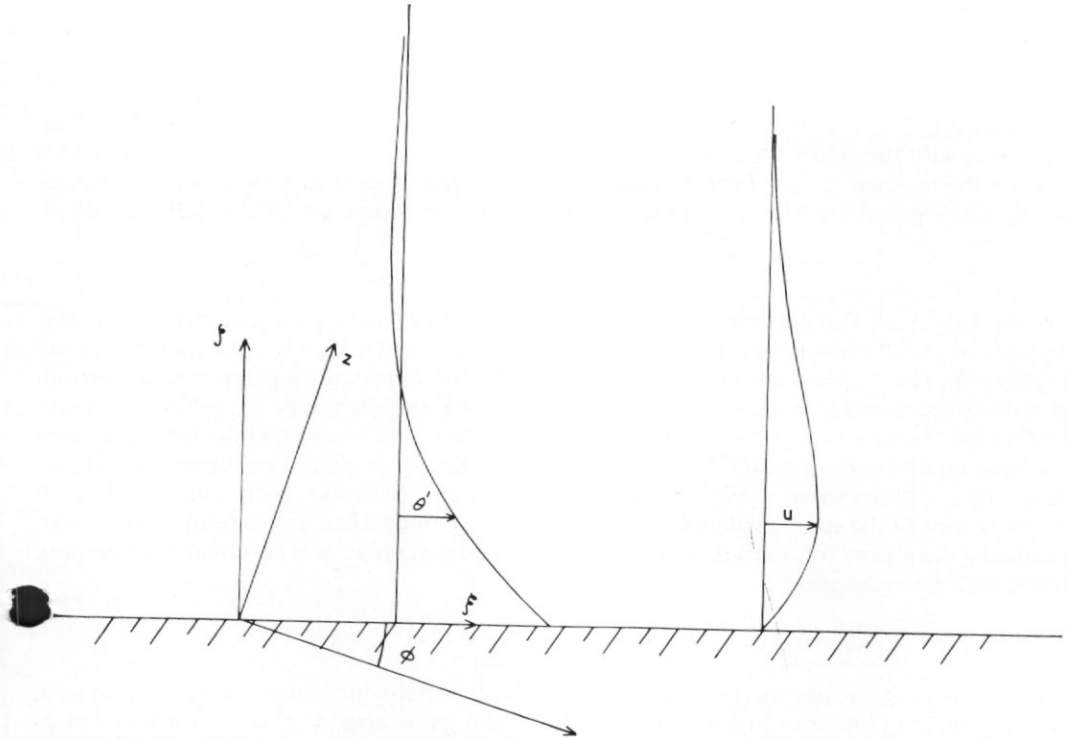

Fig. 17. Profiles of air temperature (θ) and wind speed (u) over a sloping surface from Prandtl (1952). The temperature is given by $\theta = A+Bz+\theta'(\zeta)$.

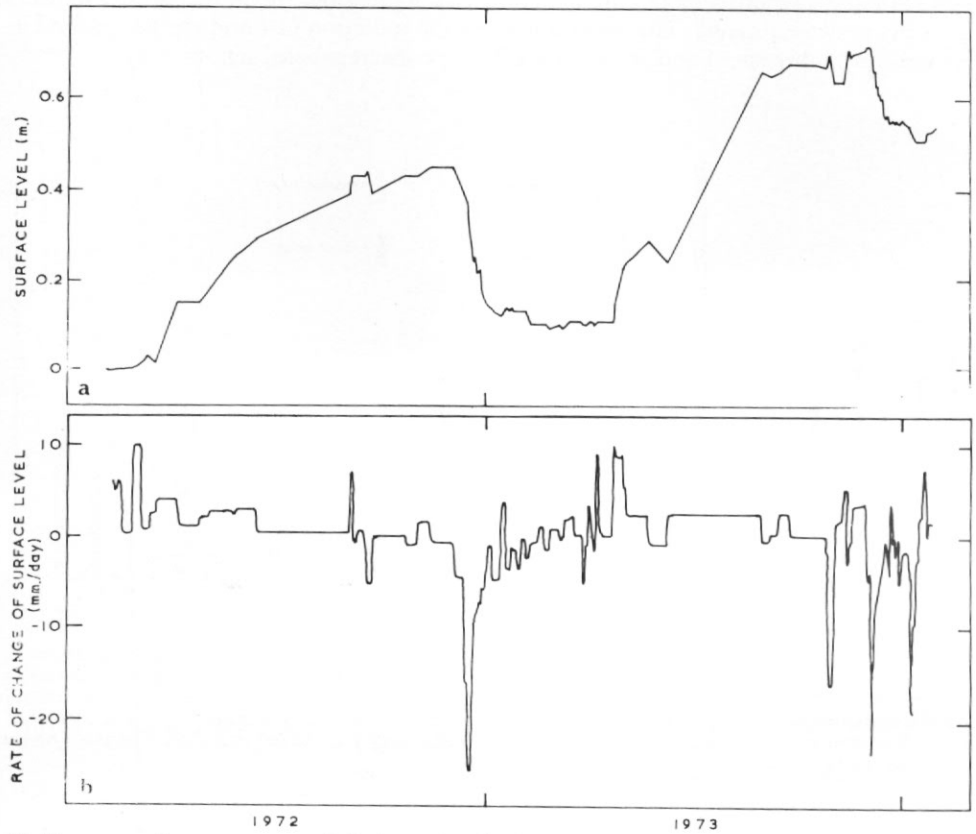

Fig. 18. Summary of measurements of glacier-surface level near the meteorological site.
a. Surface level at stake B61 (Fig. 3).
b. Average rate of change of surface level for nine stakes (Fig. 3).

A value of 0·001 m. was used for z_0 determined from logarithmic plots of wind-speed profiles. This agrees with the values found by others (Deacon, 1949, p. 92). θ_1, θ_2, q_1 and q_2 are measurements by the top two sensors for temperature and humidity, above the area affected by downslope winds. Figs. 10d and 19 show the results obtained from September 1973 to February 1974.

Melting

At the height of summer the surface layers of the glacier melted during part of the day. The level of the glacier surface was observed relative to nine stakes near the meteorological site (Fig. 3). The stakes were visited at intervals of 1 or 2 days during the melting period. The data collected are summarized in Fig. 18a. To calculate the heat used in melting, a density of 600 kg. m.$^{-3}$ was assumed midway between the densities of the snow and the ice. There may have been an error of up to 100 kg. m.$^{-3}$ because the density could not be measured directly. The results are summarized in Fig. 18b. 5-day totals are plotted in Fig. 19 for comparison with the other terms of the energy balance. An experiment was undertaken with a lysimeter to weigh a sample of the glacier surface but the presence of the lysimeter platform dominated the melting pattern and the experiment had to be abandoned.

The energy balance

The components of the energy balance during the 6 months for which measurements were most reliable are plotted in Fig. 19. In general the heat gains always exceeded the heat losses and the discrepancy was often greater than any single term. The probable explanation of the discrepancy is that the sensible and latent-heat fluxes, which were often heat sources, were over-estimated as suggested by Holmgren. Heat used in melting, which was always a heat loss, was possibly under-estimated. The uncertainties in the radiation flux and the heat stored in the glacier were probably small and would not affect the discrepancies significantly.

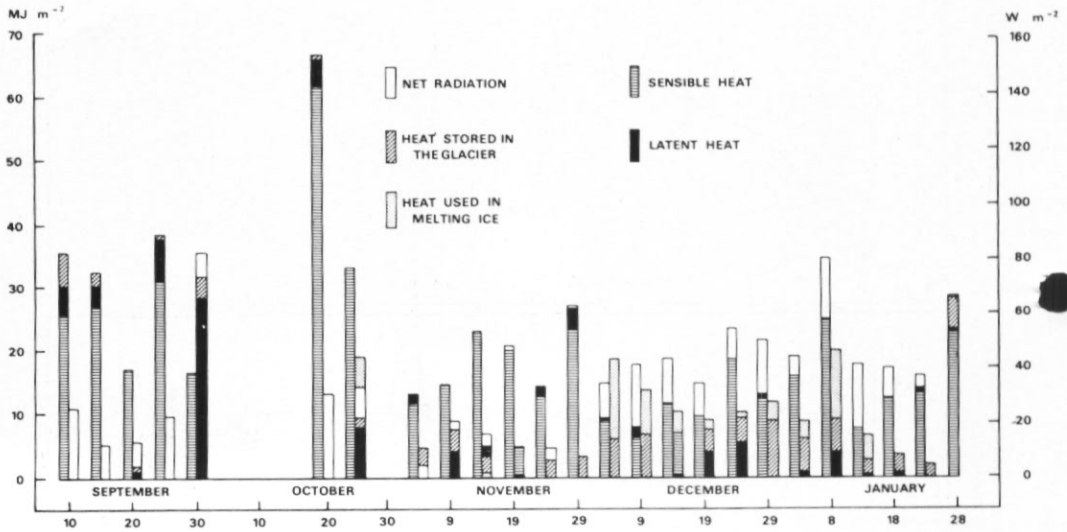

Fig. 19. 5 day totals of the components of the energy balance from September 1973 to February 1974. Each 5 day period is represented by two vertical bars, the one on the left showing heat gained by the glacier and the one on the right showing heat lost. Because energy is conserved, both bars should be the same height. Discrepancies indicate the size of errors caused by deficiencies in the theory of turbulent transfer. The scale on the right gives the total energy transferred in 5 days. The scale on the left gives the equivalent power.

Conclusions

The three balances (UNESCO/IASH, 1970, p. 13) may be simplified for Spartan Glacier, as shown in Table III.

Table III. The three balances at Spartan Glacier

Conserved quantity	*Significant components*
Mass of ice	a. Accumulation of snow. b. Flow of ice into and out of the study area. c. Melting measured directly.
Mass of water	d. Water from snow melt on the sides of the valley. e. Run-off. f. Melting (not measured).
Energy	g. Heat stored in the glacier. h. Heat used in melting ice (not measured). i. Energy from surroundings.

Term i above is the aggregate of sensible heat, latent heat and net radiation exchanged at the glacier surface. For the present purposes the relative proportions of these are irrelevant. Terms c, f and h all represent the melting. This can be measured directly as c and inferred as a check from the other two balances.

Ice balance

If the mass of ice above a reference level were determined with sufficient accuracy all over the glacier, there would be no need for a check on the ice balance. However, on Spartan Glacier densities could not be determined accurately by weighing blocks of snow. A possible alternative (McKay, 1968, p. 60–62) would be to place a radiation detector in the glacier below the depth at which changes in mass take place. The attenuation of a radioactive source placed on the surface would be proportional to the mass of ice above the sensor. Several detectors buried in the glacier could be used to calibrate conventional stake measurements. On glaciers where areas are inaccessible because of crevasses, the amount of ice flowing into or out of such areas would also have to be measured in order to determine the ice balance.

Energy balance

Measurements of energy from the surroundings (term i above) were not accurate, nor is it likely that they could ever be improved sufficiently to test the absolute accuracy of the energy-balance equation. However, the heat used in melting (term h) can be obtained from term c. Term i can then be deduced as the residual of the energy balance. The aggregate of the turbulent-transfer terms can be obtained by subtracting the net radiation, which can be measured simply, from term i. The impracticability of measuring the sensible- and latent-heat fluxes prevents further resolution of term i.

Repeated measurements of the temperature profile in the glacier over a period of say 10 years would be an indicator of long-term changes in the glacier mass budget. Measurements indicating an increase in the energy stored would imply that the glacier was warming up. In this case, the intersection of the melting-point isotherm with the glacier surface would move up the glacier and ablation would increase.

ACKNOWLEDGEMENTS

The work was carried out by the Glaciology Section of the British Antarctic Survey under the direction of Dr. C. W. M. Swithinbank. During preparations Dr. H. Lister, Mr. D. W. S. Limbert, Dr. K. A. Edwards and several members of staff of the Institute of Hydrology gave valuable advice. Many personnel of the British Antarctic Survey helped to build, supply and run the station. In particular, our thanks go to the aircraft pilots, N. Rowley and B. J. Conchie, and field assistants G. Whitworth, R. G. Tindley, S. A. Hobbs, K. F. Avery and R. W. H. Wilkins. We have used additional data gathered by G. F. Kistruck, M. R. Pearson, I. H. Rose, J. F. Bishop and F. G. Tourney. We are grateful to Mrs. P. Little, who did much of the tedious digitizing of chart records. We thank Dr. Swithinbank, Dr. D. A. Peel and Dr. C. S. M. Doake for commenting on and improving the manuscript.

MS. received 10 May 1976

REFERENCES

DALRYMPLE, P. C., LETTAU, H. H. *and* S. H. WOOLASTON. 1966. South Pole micrometeorology program: data analysis. (*In* RUBIN, M. J., *ed. Studies in Antarctic meteorology*. Washington, D.C., American Geophysical Union, 15–58.) [Antarctic Research Series, Vol. 9.]

DEACON, E. L. 1949. Vertical diffusion in the lowest layers of the atmosphere. *Q. J. R. met. Soc.*, **75,** No. 323, 89–103.

DE LA CASINIÈRE, A. C. 1974. Heat exchange over a melting snow surface. *J. Glaciol.*, **13,** No. 67, 55–72.

DUDNIK, E. E. 1971. *SYMAP*. Chicago, College of Architecture and Art, University of Illinois at Chicago Circle. [Department of Architecture Report No. 71–1.]

HAVENS, J. M., MÜLLER, F. *and* G. C. WILMOT. 1965. Comparative meteorological survey and a short term heat balance study of the White Glacier. *Axel Heiberg Island Research Reports*, Meteorology, No. 4, 68 pp.

HOLMGREN, B. 1971. On the katabatic winds over the north-west slope of the ice cap. Variations in the surface roughness. (*In* Climate and energy exchange on a sub-polar ice cap in summer. Part C. *Meddn Upps. Univ. met. Instn*, Nr. 109, 43 pp.)

LA CHAPELLE, E. R. 1969. *Field guide to snow crystals*. Seattle and London, University of Washington Press.

LETTAU, H. H. 1966. A case study of katabatic flow on the South Polar plateau. (*In* RUBIN, M. J., *ed. Studies in Antarctic meteorology*. Washington, D.C., American Geophysical Union, 1–11.) [Antarctic Research Series, Vol. 9.]

LISTER, H. *and* P. F. TAYLOR. 1961. Heat balance and ablation on an Arctic glacier. *Meddr Grønland*, **158,** No. 7, 1–54.

MCKAY, G. A. 1968. Problems of measuring and evaluating snow cover. (*In Snow hydrology*. Ottawa, Canadian National Committee for the International Hydrological Decade, 49–62.)

PEARSON, M. R. *and* I. H. ROSE. 1983. The dynamics of George VI Ice Shelf. *British Antarctic Survey Bulletin*, No. 52.

PRANDTL, L. 1952. *Essentials of fluid dynamics*. London and Glasgow, Blackie and Son.

STRETEN, N. A. *and* G. WENDLER. 1968. The midsummer heat balance of an Alaskan maritime glacier. *J. Glaciol.*, **7,** No. 51, 431–40.

UNESCO/IASH. 1970. *Combined heat, ice and water balances at selected glacier basins. A guide for compilation and assemblage of data for glacier mass balance measurements*. Paris, UNESCO/IASH. [Technical Papers in Hydrology, No. 5.]

———. 1973. *Combined heat, ice and water balances at selected glacier basins. Part II: specifications, standards and data exchange*. Paris, UNESCO/IASH. [Technical Papers in Hydrology, No. 5, Pt. 2.]

WAGER, A. C. 1982. Mapping the depth of a valley glacier by radio echo sounding. *British Antarctic Survey Bulletin*, No. 51, 111–23.

APPENDIX A

INSTRUMENTS

Sensors used to measure micro-meteorological conditions near the glacier surface are shown in Figs. 20–25, and their details are summarized in Table IV. A schematic diagram of the arrangement of sensors, recording system and power supplies is shown in Fig. 26.

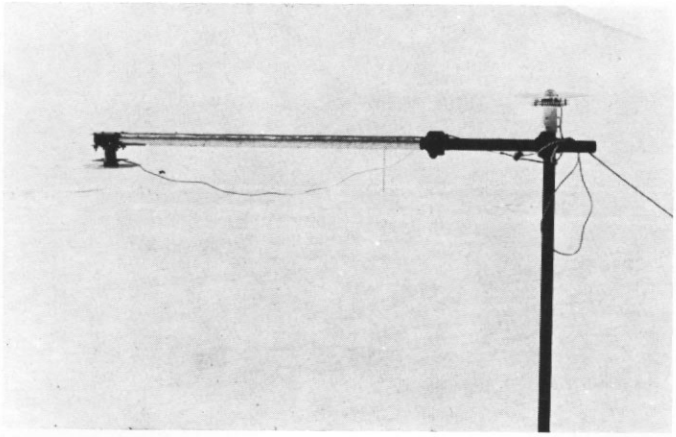

Fig. 20. Solarimeters mounted to measure the vertical components of solar radiation.

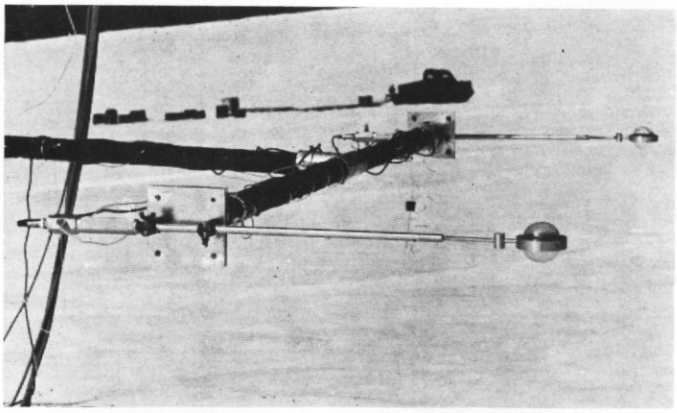

Fig. 21. Radiometers to measure net all-wave radiation.

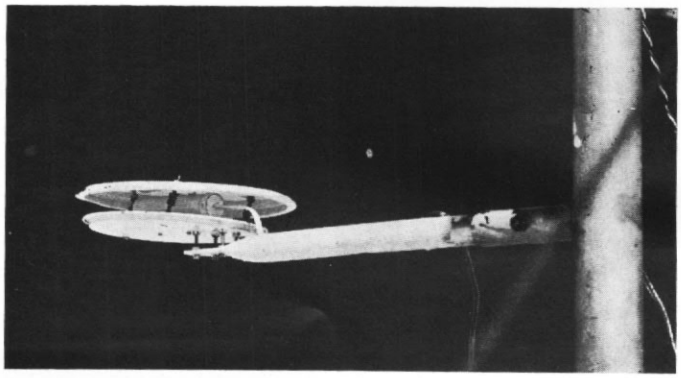

Fig. 22. Air-temperature sensor and radiation shield.

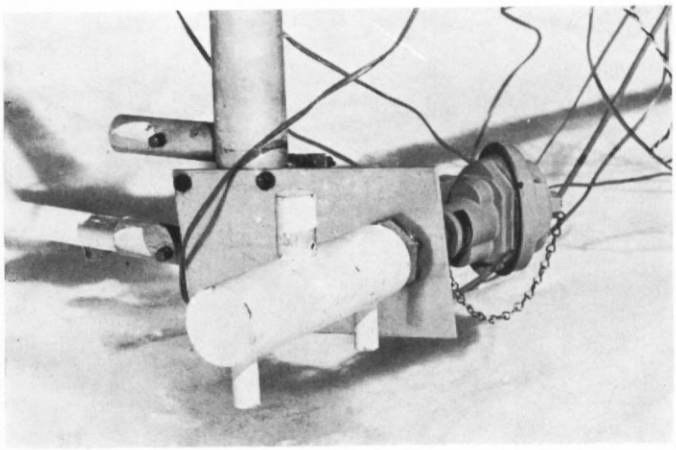

Fig. 23. Dewcel humidity sensor in shield.

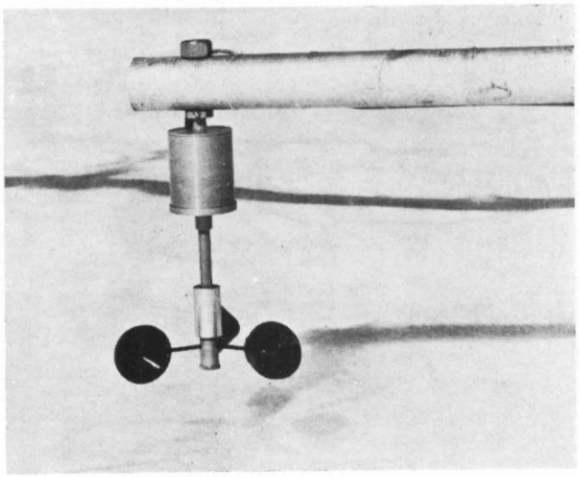

Fig. 24. Anemometer.

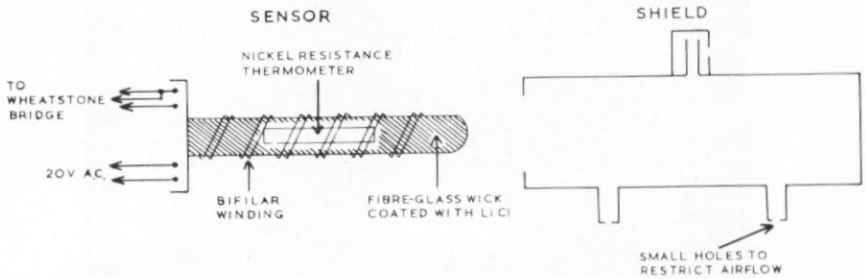

Fig. 25. Dewcel and shield.
Lithium chloride (LiCl) is hygroscopic and its electrical conductivity increases with the proportion of moisture absorbed. The alternating current flowing between the elements of the bifilar winding heats the LiCl until evaporation and absorption are in equilibrium. The equilbrium temperature is a function of the mixing ratio. The shield fits over the sensor to reduce air-flow and radiation effects.

TABLE IV. SUMMARY OF SENSORS USED TO MEASURE METEOROLOGICAL QUANTITIES

Instrument (maker)	*Parameter measured*	*Sensitivity and accuracy*	*Calibration*	*Method of increasing response time*
Porton anemometer (Spembly)	Wind speed (m. sec.$^{-1}$)	0·2 V /m. sec.$^{-1}$ Starting speed 0·2 m. sec.$^{-1}$ Accuracy $\pm$0·05 m. sec.$^{-1}$	Manufacturer's	Resistance/capacitance filter
Moll-Gorczynski solarimeter (Kipp and Zonen)	Intensity of shortwave radiation (W m.$^{-2}$)	12 μV/W m.$^{-2}$ Accuracy $\pm$5 per cent	Manufacturer's	Resistance/energy-storage device filter (energy-storage device equivalent to a large capacitor of value 1F)
Funk radiometer (CSIRO)	Intensity of net all-wave radiation (W m.$^{-2}$)	78 μV/W m.$^{-2}$ Accuracy $\pm$5 per cent	Manufacturer's	Resistance/energy-storage device filter
Dewcel (Foxboro-Yoxall)	Mixing ratio	See Appendix C Accuracy $\pm$2 per cent	Nickel resistance thermometer calibrated with respect to freezing point. Mixing ratio/element temperature from manufacturer	Air flow to sensor restricted
Platinum resistance thermometers (Sangamo-Weston)	Temperature (°C)	0·52Ω °C^{-1} Accuracy $\pm$0·1°C	Sensitivity: manufacturer's Zero point: reference to freezing point	Encapsulation of air-temperature sensor in paraffin wax Ice temperature varied slowly
Chromel-constantan thermocouples	Temperature difference (°C)	58·1 μV °C^{-1} Accuracy $\pm$0·05°C	Platinum resistance thermometers	As for platinum resistance thermometers
Speedomax W 24-channel chart recorder (Leeds and Northrup)		0 to 1 mV F.S.D. (15 channels) $-$0·5 to +0·5 mV F.S.D. (9 channels) Accuracy $\pm$0·3 per cent F.S.D.		

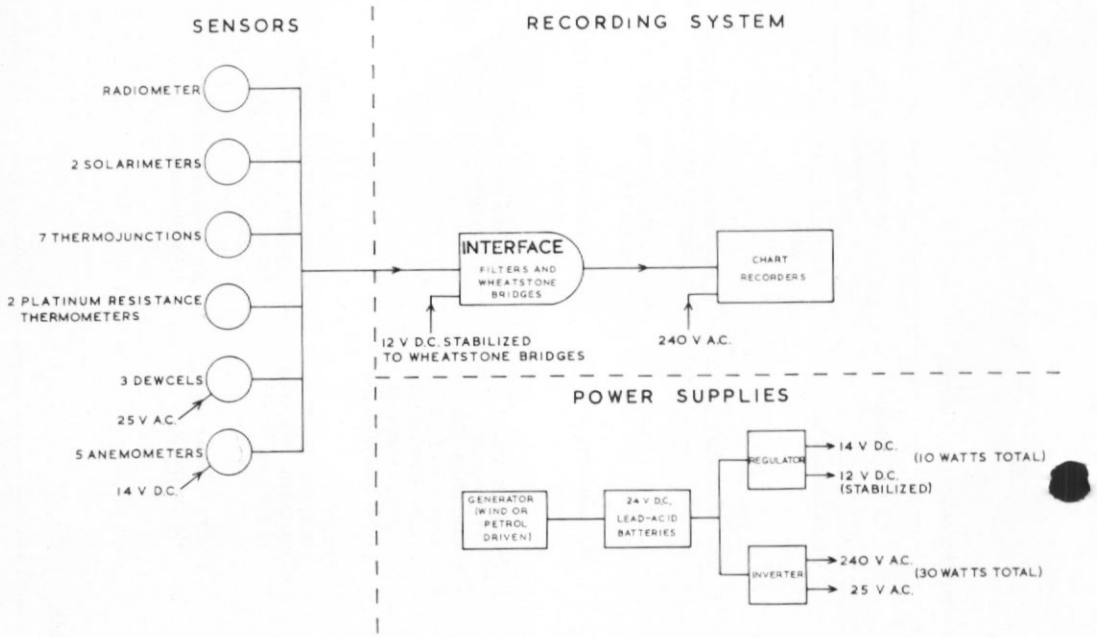

Fig. 26. Sensors, recording system and power supplies.

APPENDIX B

A Proposed Recording System

The data-recording system used in this study had shortcomings which in a future study could be avoided in the following way.

Basic requirements

i. The system must provide an output which is computer compatible to avoid the tedious digitizing of chart records.

ii. A chart record must also be provided to help in the tracing of faults and for use as a working copy. The eye, accustomed to regular patterns, can more readily detect changes than can a computer. Thus a chart record may reveal faults which are not apparent on a digital record.

iii. An independently powered clock must encode the time on both digital and chart records at, say, hourly intervals. Errors were caused by chart slipping and by incorrect time marks. With time marks at daily intervals, it was often difficult later to establish the sequence of events.

iv. The power consumption of the equipment must be as low as possible. The continuous supply of 20 W requires almost 1 tonne of petrol per year.

v. The recorders should have high sensitivity so that passive filtering of the sensor outputs can be used.

vi. For easy maintenance, the system should contain as few components as possible, preferably encapsulated units. The interface for the recorders should contain a separate plug-in circuit card for each of the sensors.

Recording

For a system that records data slowly in a remote place, paper tape has many advantages over magnetic tape Paper tape can be read in the field whereas magnetic tape cannot. Most magnetic tape data loggers only check information before it is sent to the tape; they do not check the contents of the tape. A read-after-write magnetic tape deck requires a lot of power; an intermittent paper-tape punch does not. Any computer can read paper tape punched in binary code, whereas magnetic tapes generally require a special unit. 8 hole binary code gives 1/4 per cent precision or 1 per cent with a parity check. The channel-switching mechanism of a multi-channel potentiometric chart recorder can be used to switch the sensor outputs to the digital recorder. The response time of the sensors should be approximately 30 min. and the data should be sampled at 5 min. intervals. An accurate representation of the 30 min. mean will be obtained and will not be degraded if the occasional sample cannot be read.

APPENDIX C
DATA PROCESSING
Energy balance

Digitizing and checking

A schematic diagram of how the data were processed is shown in Fig. 27. The chart record was laid on a digitizing table and the trace of each sensor was followed with the digitizing pointer. The coordinates of the pointer at 1 mm. intervals were automatically recorded on either magnetic or punched paper tape. The tape was later read by a computer program. The coordinates measured on the plotting table were converted to time in minutes and recorder scale units (10 μV) by referring to a file derived from time marks on the charts. Sample values at 5 min. intervals were calculated by interpolating between the digitized points (Fig. 28). Interpolation to 5 min. intervals was convenient for the following reasons:

i. Position in the data base (Fig. 29) and time were related simply so that data could be located efficiently.
ii. Questionable digitized points could be ignored and the gaps filled by interpolation. This was acceptable for at least one missing digitized point because of the long response time of the sensors.
iii. It was possible to work faster when digitizing slowly varying traces by increasing the interval between digitized points.

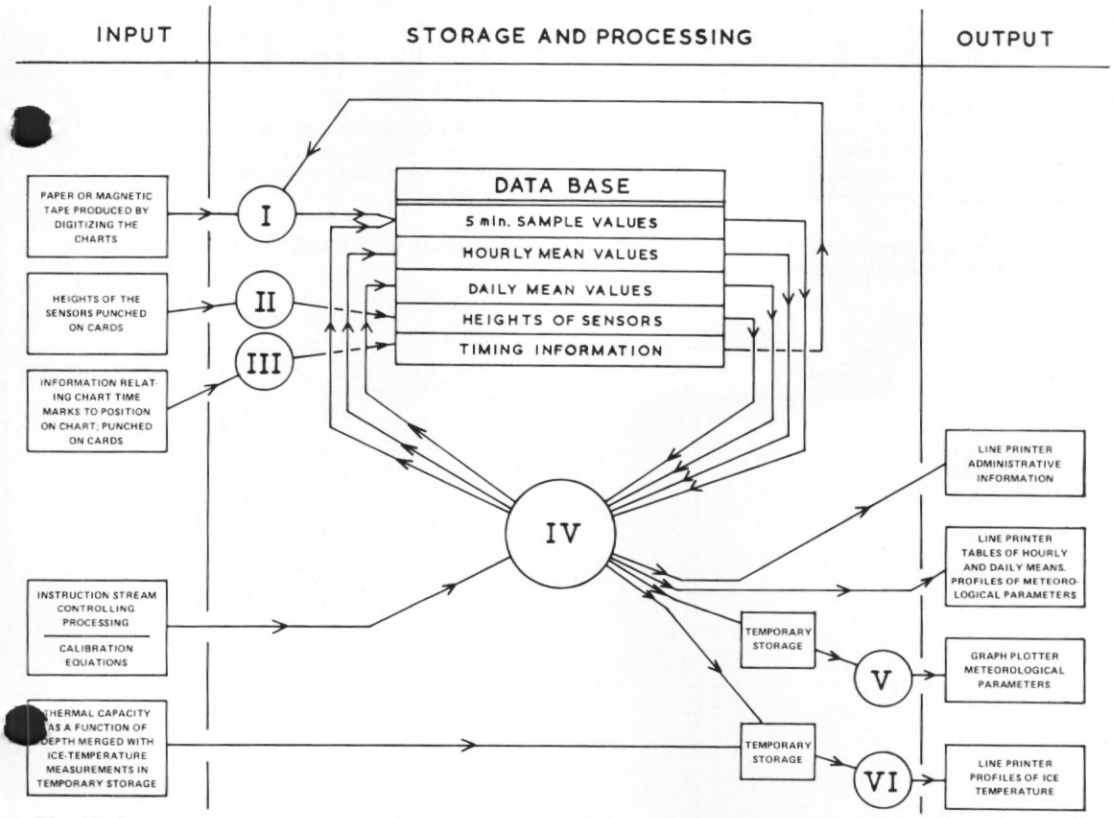

Fig. 27. Schematic diagram of data processing. Computer programs performed the following operations:

I. Filed 5 min. sample values from digitized data.
II. Checked and filed heights of the sensors.
III. Checked and filed correlation between time marks and position on chart.
IV. (i) Edited sample values, converted them to SI units and performed simple arithmetic.
(ii) Calculated and edited hourly and daily means.
(iii) Printed data in tabular form for reference.
(iv) Prepared data for plotting on the graph plotter by another program.
(v) Prepared data from which another program calculated the amount of heat stored in the glacier.
(vi) Plotted profiles of meteorological parameters by fitting curves.
(vii) Calculated sensible- and latent-heat fluxes.
V. Produced graphs from coordinate data supplied by another program (para IV. (iv) above).
VI. Integrated between two curves fitted to ice temperature as a function of depth to calculate the amount of heat stored in the glacier.

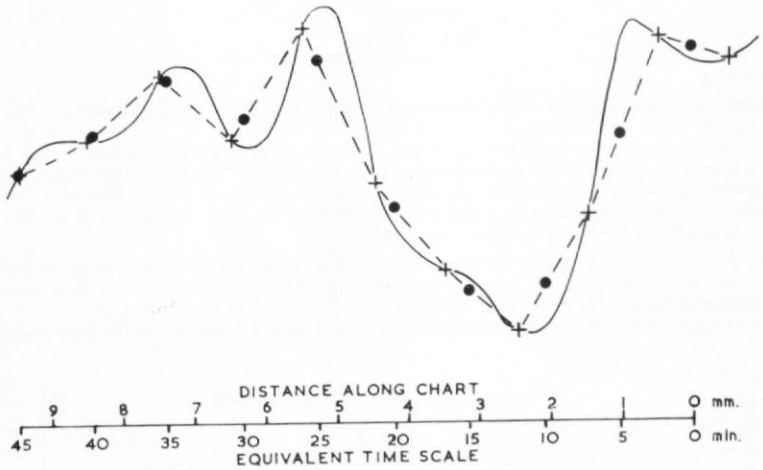

Fig. 28. Interpolation of 5 min. values from digitized points. The solid line represents the original trace on the chart. + symbols mark the points automatically digitized at 1 mm. intervals. Solid circles represent 5 min. sample values interpolated along the pecked lines. The long response time of the sensors ensured that discrepancies between interpolated points and the trace were small.

The sample values were plotted to form an image of the original chart. Errors could be quickly detected by laying the image over the original.

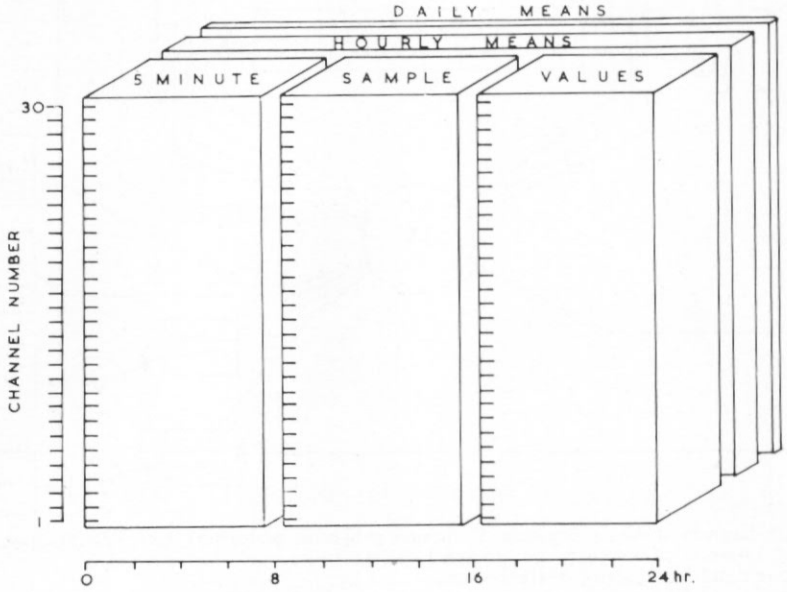

Fig. 29. Storage of data for 1 day.

	Resolution	*Storage density* bits $h.^{-1}$	bits per data point
5 min. sample value	1 part in 250	105·2	8·8
Hourly mean	1 part in 2^{24} ($\sim 10^7$)	35·1	25·1
Daily mean	1 part in 2^{24} ($\sim 10^7$)	11·6	283

Programs were written in PL/I for an IBM 370 computer.

The data base

The data were collected into a data base which was easily accessible by computer. The data base could be visualized as a three-dimensional matrix (Fig. 29). Data were referred to by three indices: time, channel number and type of data. The time scale was in minutes elapsed from a reference time and the smallest increment used was 5 min., the interval between sample values. The channel number was a label identifying data from a particular sensor. Channels also contained-data such as albedo and sensible-heat flux, which were indirectly derived from the sensors. The three types of data were 5 min., hourly and daily means of the measured micro-meteorological parameters. Sample values at 5 min. intervals contained all the information available from the charts. This part of the data base was stored compactly and was unpacked each time it was used. Hourly means, the average of 12 sample values, were used for most of the calculations. They were not stored as compactly as the sample values and could therefore be obtained quickly. The daily mean, maximum and minimum were taken from 288 sample values.

Conversion to SI units

After sample values had been checked, they were converted from chart-recorder scale units (10 μV) to SI units. The conversion was with one exception

$$C = a_0 + a_1 U,$$

where U was the parameter value in chart-recorder scale units, C was the value in SI units and a_0 and a_1 were derived from the calibration data. The Dewcel humidity sensors did not have a linear calibration equation. Curves of the form

$$C = \exp(a_0 + a_1 R + a_2 R^2)$$

were fitted to data provided by the makers (Foxboro-Yoxall). R was the Dewcel element resistance. Values obtained were

$$a_0 = -81{\cdot}8532,$$
$$a_1 = 0{\cdot}546649,$$
$$a_2 = -0{\cdot}858653 \times 10^{-3}.$$

R was given by

$$R = b_0 + b_1 U$$

where b_0 and b_1 were the zero point and sensitivity of an off-balance Wheatstone bridge and U was the recorded output value of the bridge.

Calculation of Richardson numbers

We interpolated between hourly mean values of wind speed, air temperature and humidity along a curve which passed through the values and had a continuous derivative. A set of cubic curves each fitted between a pair of adjacent values was used (Fig. 16). Richardson numbers were calculated (Equation (5)) using the derivatives of the fitted curves.

Calculation of energy fluxes

Of the five components of the total energy flux, only the net radiation flux was available directly from the data base. Sensible- and latent-heat fluxes were calculated by substituting hourly mean temperatures and humidities from the data base into Equations (6) and (7). The wind speed u_2 at the upper height z_2 was interpolated from the hourly mean wind speeds. The heat stored in the glacier was calculated in two stages. Daily mean ice temperatures at three levels and the estimated surface temperature were obtained from the data base. The heat capacities per unit volume of the snow and ice layers were included and a second computer program fitted the temperature/depth curve (Equation (2)). The integral (Equation (1)) was calculated numerically to give the amount of heat stored in the glacier.

Errors

The sample values were plotted to reproduce the chart. Gross errors in digitizing were detected by superimposing this on the original. Errors were introduced into the sample values when they were converted to SI units. The errors came from uncertainties in the calibration of the sensors (Table IV in Appendix A). Zero drift of the recorders was taken into account and the conversion was done with six-digit precision. Errors caused by failure to follow the traces on the charts were probably averaged out in the hourly means, which were used for most of the calculations. Sample values were stored with a resolution, in the worst case, of 0·25 per cent of chart-recorder full scale, the same as the accuracy of the chart recorders. Daily and hourly means calculated during periods when measurements were missing were biased. This was not serious for the hourly means because the parameters changed sufficiently slowly for a few values to give a reasonable approximation. Daily means, where the bias was serious, were used only in calculating the net radiation over 5-day periods. Daily means of net radiation were not used where the measurements were discontinuous.

Only the temperature measurements could be tested for self-consistency. The difference between the temperatures at the ends of the chain (Fig. 11) was calculated independently from the resistance-thermometer measurements and also from the thermocouple measurements. A systematic difference of 0·7° C was found on analysing a sample. This difference was distributed between the resistance-thermometer sample values.

Recommendations

Computer reduction was used because of the large amount of data. Graphical presentations of data (Fig. 9) and profiles (Fig. 16) were much more understandable than tables of numbers. The use of a computer involved a lot of work in designing, programming and creating the data base before the analysis could be started. In future work of this kind an existing program package should be used. The inconveniences of a package designed for commercial use may be preferable to the work involved in writing computer programs. Measurements must be compatible with the package chosen. The method by which data are put into the computer should be considered carefully. Digitizing analogue records, as was done here, was expensive and took a long time.

Ice balance

Data storage

Over 4,000 measurements of stake length exposed were stored in the ice-balance data base. The method of storage took account of extensions of stakes and the occasional discontinuity caused by a stake melting out. The measurements of stake length exposed were converted to heights of the glacier surface. The coordinates of each stake were also stored.

Maps of change of surface level

Maps of change of surface level with time (Figs. 2 and 4) were made using a computer program (Dudnik, 1971). The height of the surface for each of two dates was obtained from the data base using linear interpolation between measurements. The total change of volume was calculated by measuring the area between lines of equal accumulation.